



Few Body Systems in Condensed Matter Physics



Roman Ya. Kezerashvili



***New York City College of Technology
Graduate School and University Center
The City University of New York***



International School and Conference on Functional Materials for Modern Technologies

ISCFMMT 2022

Batumi Shota Rustaveli State University, Batumi, Georgia October 1-7 2022

ISCFMMT 2022, Batumi, Georgia October 3, 2022

Consideration two-, three- and four-body systems in condense matter physics

- Study negatively and positively charged trions in bulk material using Faddeev equation.
- To develop the theoretical approach for description of trions in monolayer transition metal dichalcogenides MoS_2 , $MoSe_2$, WS_2 , WSe_2 within method of hyperspherical functions.
- To study the dependence of trions binding energies on the of dielectric screening and space confinement.
- To understand the origin of the difference of binding energies of negatively and positively charged trions

3D → 2D → 1D

The Schrödinger equation for a few particle in *3D*, *2D* and *1D* configuration space reads

$$\left({}^{jD}T + \sum_{i < k} {}^{jD}V(r_{ik}) \right) \Psi_{jD} = E_{jD} \Psi_{jD}$$

where index $j = 3, 2, 1$ presents the dimensionality of the space and the position vectors \mathbf{r} are defined in the jD space.

$${}^{jD}T = -\frac{\hbar^2}{2m_A} \Delta_A - \frac{\hbar^2}{2m_B} \Delta_B - \frac{\hbar^2}{2m_C} \Delta_C$$

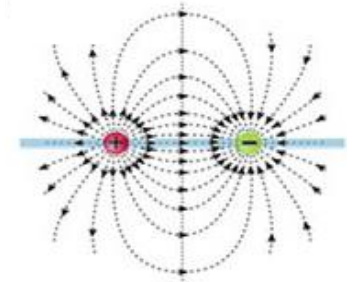
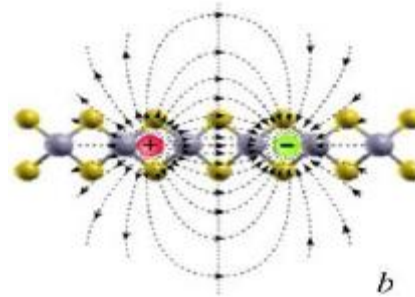
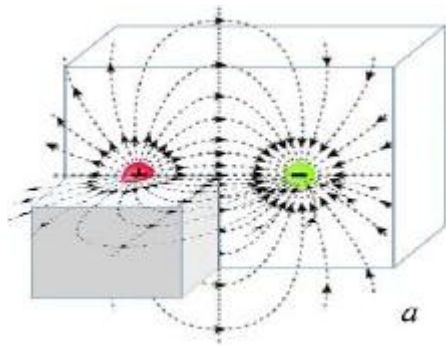
is a three-body kinetic energy operator

$$E_{jD} = \langle {}^{jD}T \rangle + \left\langle \sum_{i < k} V(r_{ik}) \right\rangle$$

The expectation value for the ground state energy

The later expression could be viewed as the sum of the average value of the operators of kinetic and potential energies in *3D*, *2D* and *1D* configuration space, respectively, obtained by using the corresponding eigenfunction of few particles in *3D*, *2D* and *1D configuration spaces*.

Interaction: 3D → 2D → 1D



$${}^3D V(r) = \frac{ke^2}{\epsilon r}$$



Coulomb Potential

Dielectric constant describes the polarization of 3D medium

$${}^2D V(r) = \frac{\pi ke^2}{(\epsilon_1 + \epsilon_2)\rho_0} \left[H_0\left(\frac{r}{\rho_0}\right) + Y_0\left(\frac{r}{\rho_0}\right) \right]$$

Rytova-Keldysh potential

Describes the Coulomb interaction screened by the polarization of the electron orbitals in the 2D lattice.

- N. S. Rytova, *Proc. MSU Phys., Astron.* 3, 30 (1967)
- L. V. Keldysh, *JETP Lett.* 29, 658 (1979).

J. Javanainen, Phys. Rev. A 38, 3430 (1988)

$${}^1D V(z) \sim A(z + r_0)^{-1}$$

$${}^1D V(z) = \frac{\pi ke^2}{\epsilon(a)} \frac{A}{z - z_0}$$

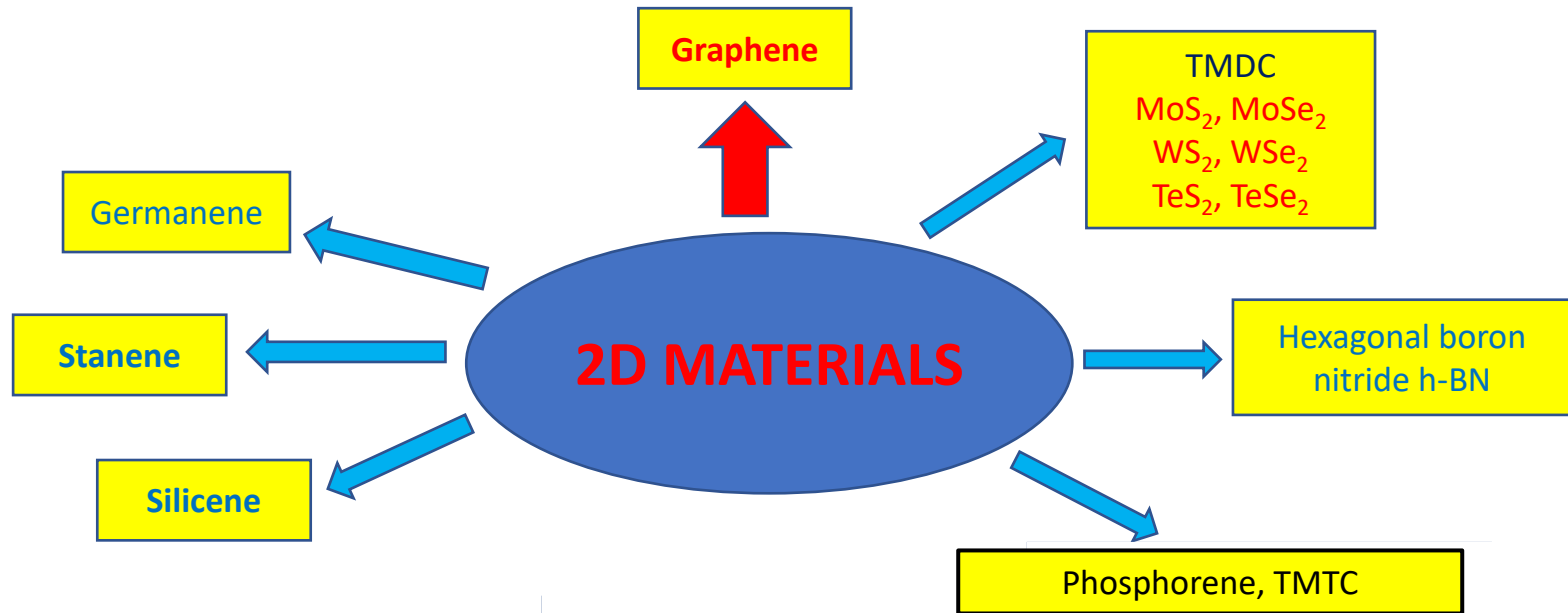
Cusp-type potential in a 1D system

Dielectric constant depends on a radius a of a nanowire

$${}^1D V(z) \sim (z^2 + a^2)^{-1/2}$$

Parameters A and r_0 are determined self-consistently by employing the eigenfunctions of the lateral confinement of electrons and holes.

Zoo of 2D Materials

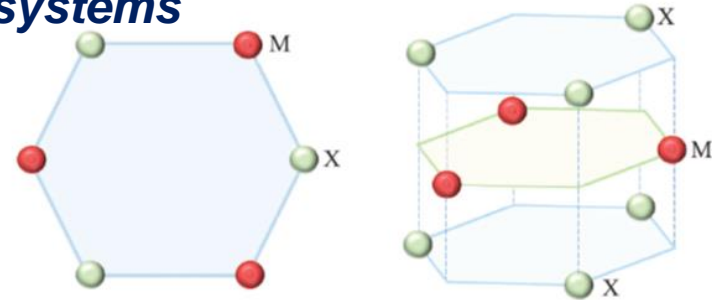


These materials are the two-dimensional allotropic forms of the corresponding **Chemical element**

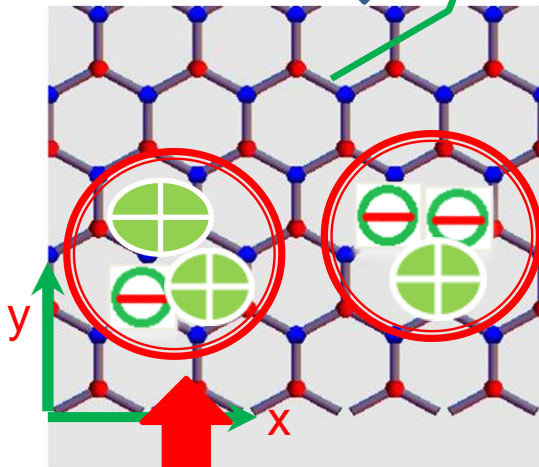
Two Dimensional Transition Metal Dichalcogenide

Atomic layers of hexagonal Transition Metal Dichalcogenides (TMDC) represent a new class of systems

Top view on the hexagonal lattice of MoS_2 lying in the xy plane



Positive and Negative Trion Complexes



2D TMDC

MoS_2
 $MoSe_2$
 $MoTe_2$

WS_2
 WSe_2
 WTe_2

22 Ti Titanium 47.867	23 V Vanadium 50.9415	24 Cr Chromium 51.9961
40 Zr Zirconium 91.224	41 Nb Niobium 92.90638	42 Mo Molybdenum 95.94
72 Hf Hafnium 178.49	73 Ta Tantalum 180.9479	74 W Tungsten 183.84

16 S Sulfur 32.066
34 Se Selenium 78.96
52 Te Tellurium 127.60

X^+

Lampert, Phys. Rev. Lett. 1, 450(1958).
Kheng, et al., Phys. Rev. Lett. 71, 1752 (1993).

Charge-charge Interaction in 2D Configuration Space

The effective charge-charge potential that describes the Coulomb interaction screened by the polarization of the electron orbitals in the 2D lattice reads

$$V_{ij}(r) = \frac{\pi k q_i q_j}{2\epsilon \rho_0} \left[H_0\left(\frac{r}{\rho_0}\right) - Y_0\left(\frac{r}{\rho_0}\right) \right]$$

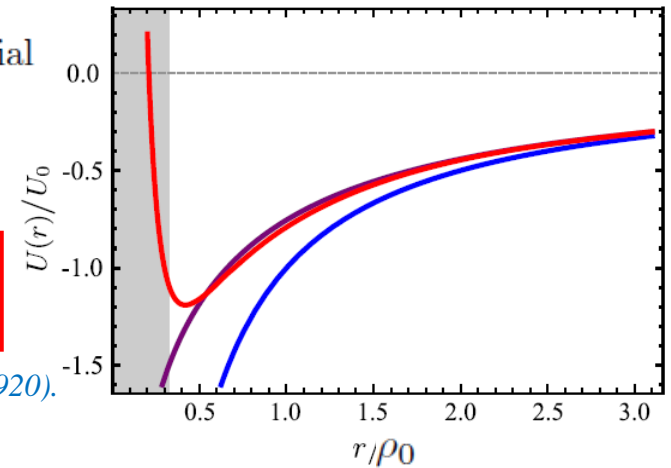
$H_0\left(\frac{r}{\rho_0}\right)$ and $Y_0\left(\frac{r}{\rho_0}\right)$ are the Struve function and Bessel function of the second kind

$\rho_0 = \frac{2\pi \chi_{2D}}{\kappa}$ is the screening length. $\kappa = (\epsilon_1 + \epsilon_2)/2$ describes the surrounding dielectric environment

In vacuum ($\epsilon_1 = \epsilon_2 = 1$), $\rho_0 = 2\pi \chi_{2D}$. Exhibiting nonlocal macroscopic screening which arises in 2D systems.
Cudazzo, et al, PRB 84, (2011).

$$V_{ij}(r) = \begin{cases} \frac{kq_i q_j}{\epsilon r}, & \text{when } r \gg \rho_0, \text{ Coulomb potential,} \\ \frac{kq_i q_j}{\epsilon \rho_0} \left[\ln\left(\frac{r}{2\rho_0}\right) + \gamma \right], & \text{when } r \ll \rho_0, \text{ Logarithmic potential} \end{cases}$$

Molas, et al. PRL 123, 136801 (2019)

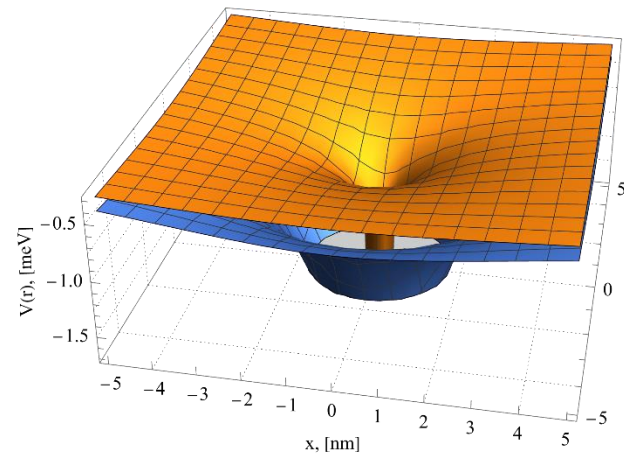


Modified Kratzer potential

$$V(r) = \frac{kq_i q_j}{\rho_0} \left(\frac{\rho_0}{r} - g^2 \frac{\rho_0^2}{r^2} \right)$$

Kratzer, Zeitschrift fur Physik 3, 289 (1920).

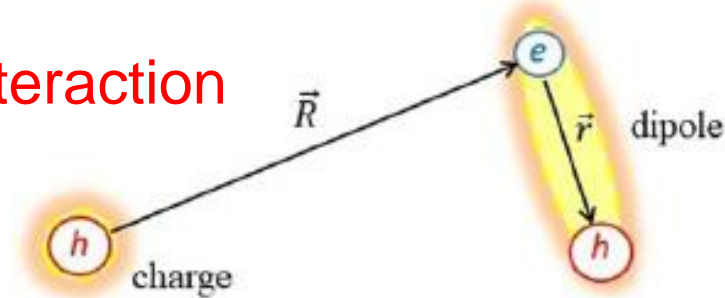
Rytova-Keldysh (purple curve), Coulomb (blue curve), and Kratzer potential (red curve), as a function of dimensionless parameter $\frac{r}{\rho_0}$



- Coulomb Potential
- Rytova-Keldysh Potential

Charge-Dipole and Dipole-Dipole Interactions in 2D materials

Charge-Dipole interaction



Schematics for the charge-dipole interactions in 2D configuration space.

System of three or four charged particle interact via 2D Keldysh-Rytova potential

$$\Rightarrow V(R) = -\frac{\pi k e^2}{2\kappa \rho_0} \left[H_0\left(\frac{R}{\rho_0}\right) - Y_0\left(\frac{R}{\rho_0}\right) \right]$$

$$V_{cd}(\mathbf{R}) = \frac{\pi k e}{2\kappa \rho_0} \left[H_{-1}\left(\frac{R}{\rho_0}\right) - Y_{-1}\left(\frac{R}{\rho_0}\right) \right] \frac{\mathbf{R} \cdot \mathbf{d}}{\rho_0 \hbar} \quad \text{Kezerashvili \& Kezerashvili PRB 105, 205416 (2022)}$$

Let prove this

$$V_{cd}(\mathbf{R}) \equiv V_{eh}(R) + V_{hh}(|\mathbf{R} + \mathbf{r}|)$$

$$= -\frac{\pi k e^2}{2\kappa \rho_0} \left[H_0\left(\frac{R}{\rho_0}\right) - Y_0\left(\frac{R}{\rho_0}\right) \right]$$

$$+ \frac{\pi k e^2}{2\kappa \rho_0} \left[H_0\left(\frac{|\mathbf{R} + \mathbf{r}|}{\rho_0}\right) - Y_0\left(\frac{|\mathbf{R} + \mathbf{r}|}{\rho_0}\right) \right]$$

$$|\mathbf{R} + \mathbf{r}| = R \sqrt{1 + \frac{2\mathbf{R} \cdot \mathbf{r}}{R^2} + \frac{r^2}{R^2}}$$

$$\text{For } R \gg r \left(1 + \frac{2\mathbf{R} \cdot \mathbf{r}}{R^2} + \frac{r^2}{R^2}\right)^{1/2} \simeq$$

$$\simeq 1 + \frac{1}{2} \left(\frac{2\mathbf{R} \cdot \mathbf{r}}{R^2} + \frac{r^2}{R^2} \right)$$

$$V_{\text{cd}}(\mathbf{R}) = -\frac{\pi k e^2}{2\kappa \rho_0} \left[H_0\left(\frac{R}{\rho_0}\right) - Y_0\left(\frac{R}{\rho_0}\right) \right]$$

$$+ \frac{\pi k e^2}{2\kappa \rho_0} \left[H_0\left(\frac{R}{\rho_0} \left[1 + \frac{\mathbf{R} \cdot \mathbf{r}}{R^2} \right] \right) - Y_0\left(\frac{R}{\rho_0} \left[1 + \frac{\mathbf{R} \cdot \mathbf{r}}{R^2} \right] \right) \right]$$

$$H_0\left(\frac{R}{\rho_0} \left[1 + \frac{\mathbf{R} \cdot \mathbf{r}}{R^2} \right] \right) \simeq H_0\left(\frac{R}{\rho_0}\right) + H_0'(x)|_{x=R/\rho_0} \frac{R}{\rho_0} \frac{\mathbf{R} \cdot \mathbf{r}}{R^2}$$

$$= H_0\left(\frac{R}{\rho_0}\right) + H_{-1}\left(\frac{R}{\rho_0}\right) \frac{R}{\rho_0} \frac{\mathbf{R} \cdot \mathbf{r}}{R^2},$$

$$Y_0\left(\frac{R}{\rho_0} \left[1 + \frac{\mathbf{R} \cdot \mathbf{r}}{R^2} \right] \right) \simeq Y_0\left(\frac{R}{\rho_0}\right) + Y_0'(x)|_{x=R/\rho_0} \frac{R}{\rho_0} \frac{\mathbf{R} \cdot \mathbf{r}}{R^2}$$

$$= Y_0\left(\frac{R}{\rho_0}\right) + Y_{-1}\left(\frac{R}{\rho_0}\right) \frac{R}{\rho_0} \frac{\mathbf{R} \cdot \mathbf{r}}{R^2}.$$

Finally charge-dipole interaction

$$V_{\text{cd}}(\mathbf{R}) = \frac{\pi k e}{2\kappa \rho_0} \left[H_{-1}\left(\frac{R}{\rho_0}\right) - Y_{-1}\left(\frac{R}{\rho_0}\right) \right] \frac{\mathbf{R} \cdot \mathbf{d}}{\rho_0 R}.$$

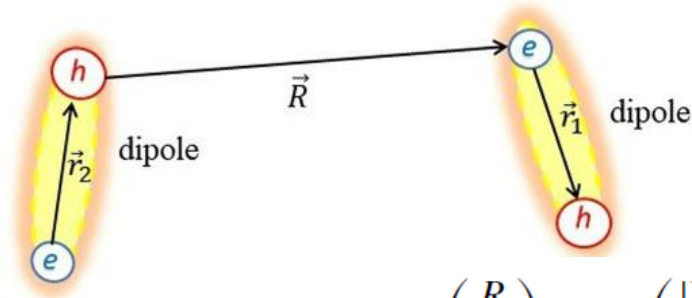
Asymptotic

$$\xrightarrow{R \rightarrow \infty} -\frac{k e}{\kappa} \frac{\mathbf{R} \cdot \mathbf{d}}{R^3}$$

Charge-Dipole interaction for Coulomb potential in 3D

$$\xrightarrow{\hspace{2cm}} V_{\text{cd}}^C(\mathbf{R}) = -\frac{k e}{\kappa} \frac{\mathbf{R} \cdot \mathbf{d}}{R^3}$$

Dipole-Dipole interaction



Schematics for the dipole-dipole interactions in 2D configuration space.

$$V_{dd}(\mathbf{R}) = V_{hd}\left(\frac{R}{\rho_0}\right) + V_{ed}\left(\frac{|\mathbf{R} + \mathbf{r}_2|}{\rho_0}\right).$$

$$V_{dd}(\mathbf{R}) = \frac{\pi k e^2}{2\kappa \rho_0^2} \left[H_{-1}\left(\frac{R}{\rho_0}\right) - Y_{-1}\left(\frac{R}{\rho_0}\right) \right] \frac{\mathbf{R} \cdot \mathbf{r}_1}{R} - \frac{\pi k e}{2\kappa \rho_0^2} \left[H_{-1}\left(\frac{|\mathbf{R} + \mathbf{r}_2|}{\rho_0}\right) - Y_{-1}\left(\frac{|\mathbf{R} + \mathbf{r}_2|}{\rho_0}\right) \right] \frac{(\mathbf{R} + \mathbf{r}_2) \cdot \mathbf{r}_1}{|\mathbf{R} + \mathbf{r}_2|}$$

$$V_{dd}(R) = -\frac{\pi k}{2\kappa \rho_0} \left\{ \left[H_{-1}\left(\frac{R}{\rho_0}\right) - Y_{-1}\left(\frac{R}{\rho_0}\right) \right] \frac{\mathbf{d}_1 \cdot \mathbf{d}_2}{\rho_0 R} + \left[H_{-2}\left(\frac{R}{\rho_0}\right) - Y_{-2}\left(\frac{R}{\rho_0}\right) \right] \frac{\mathbf{R} \cdot \mathbf{d}_1 \mathbf{R} \cdot \mathbf{d}_2}{\rho_0^2 R^2} \right\}$$

$$V_{dd}(\mathbf{R}) \xrightarrow{R \rightarrow \infty} \frac{k}{\kappa} \frac{1}{R^3} \left[\mathbf{d}_1 \cdot \mathbf{d}_2 - 3 \frac{(\mathbf{R} \cdot \mathbf{d}_1)(\mathbf{R} \cdot \mathbf{d}_2)}{R^2} \right]$$

For comparison the dipole-dipole interaction in 3D configuration space for the Coulomb potential has the following form

$$V_{dd}^C(\mathbf{R}) = \frac{k}{\kappa} \frac{1}{R^3} \left[\mathbf{d}_1 \cdot \mathbf{d}_2 - 3 \frac{(\mathbf{R} \cdot \mathbf{d}_1)(\mathbf{R} \cdot \mathbf{d}_2)}{R^2} \right]$$

Dipole-Dipole Interaction in 2D materials

$$V_{dd}(R) = -\frac{\pi k}{2\kappa\rho_0} \left\{ \left[H_{-1}\left(\frac{R}{\rho_0}\right) - Y_{-1}\left(\frac{R}{\rho_0}\right) \right] \frac{\mathbf{d}_1 \cdot \mathbf{d}_2}{\rho_0 R} + \left[H_{-2}\left(\frac{R}{\rho_0}\right) - Y_{-2}\left(\frac{R}{\rho_0}\right) \right] \frac{\mathbf{R} \cdot \mathbf{d}_1 \mathbf{R} \cdot \mathbf{d}_2}{\rho_0^2 R^2} \right\}$$

Asymptotic

Dipole-Dipole interaction for Coulomb potential in 3D

$$V_{dd}(\mathbf{R}) \xrightarrow{R \rightarrow \infty} \frac{k}{\kappa} \frac{1}{R^3} \left[\mathbf{d}_1 \cdot \mathbf{d}_2 - 3 \frac{(\mathbf{R} \cdot \mathbf{d}_1)(\mathbf{R} \cdot \mathbf{d}_2)}{R^2} \right]$$

$$V_{dd}^C(\mathbf{R}) = \frac{k}{\kappa} \frac{1}{R^3} \left[\mathbf{d}_1 \cdot \mathbf{d}_2 - 3 \frac{(\mathbf{R} \cdot \mathbf{d}_1)(\mathbf{R} \cdot \mathbf{d}_2)}{R^2} \right]$$

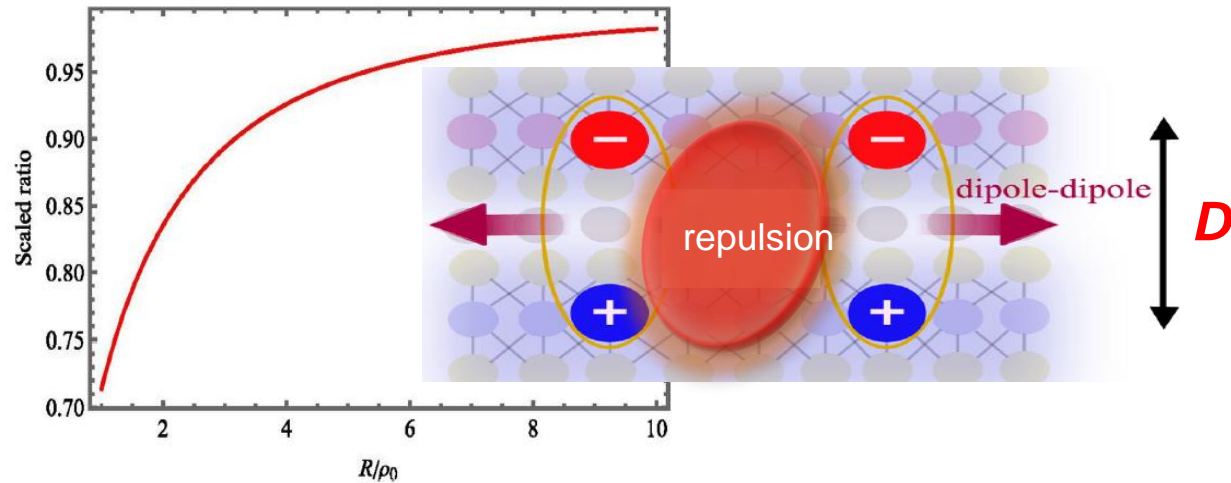
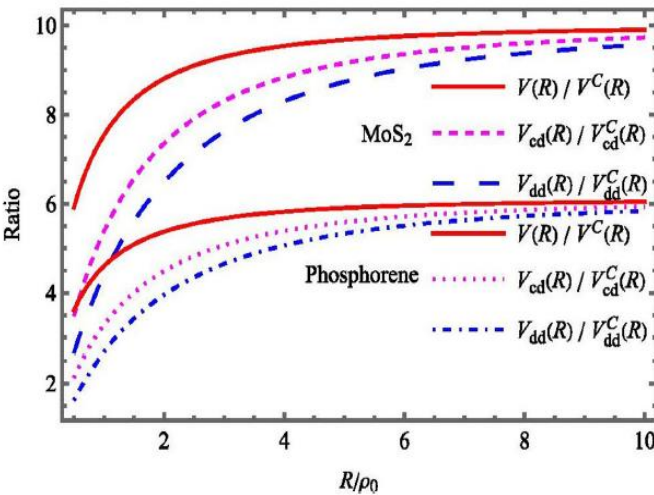
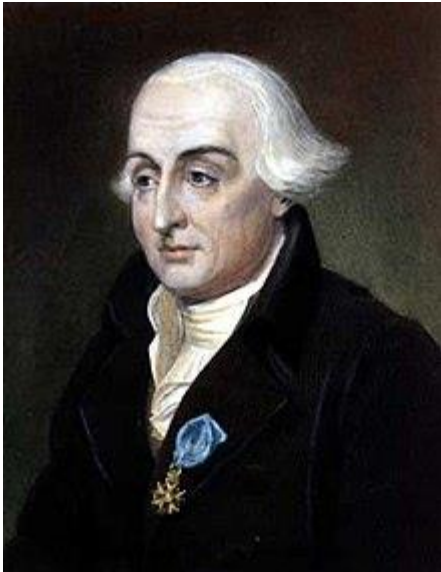


FIG. 2. Left panel: The ratios of effective 2D (1) and Coulomb potentials, charge-dipole interaction V_{cd} in 2D configuration space, and V_{cd}^C for bulk materials and the second factors of the dipole-dipole interaction in a monolayer and bulk material. Calculations are performed for the phosphorene and MoS₂. Right panel: The universal dependence of the ratio of V_{cd}/V_{cd}^C and $V(R)/V^C(R)$ on R/ρ_0 for any 2D material.

Two- and Three-body problem in Classical Physics

Joseph-Louis Lagrange
1736 - 1813



Lagrange was an Italian mathematician and astronomer later naturalized French. He made significant contributions to the fields of analysis, number theory and both classical and celestial mechanics.

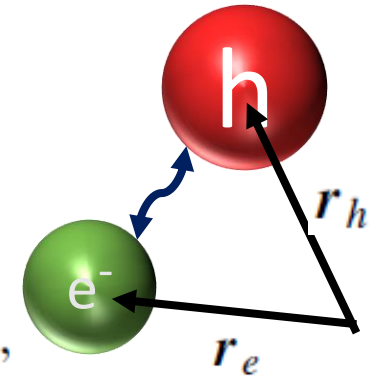
Philosophy of Two-body Problem: Exciton

The exciton is the bound state of the electron and hole.

We focus on the Mott-Wannier excitons

The Schrödinger equation for an interacting electron and hole reads:

$$\left[\frac{-\hbar^2}{2m_e} \nabla_e^2 + \frac{-\hbar^2}{2m_h} \nabla_h^2 + V(\mathbf{r}_e, \mathbf{r}_h) \right] \psi(\mathbf{r}_e, \mathbf{r}_h) = E \psi(\mathbf{r}_e, \mathbf{r}_h),$$



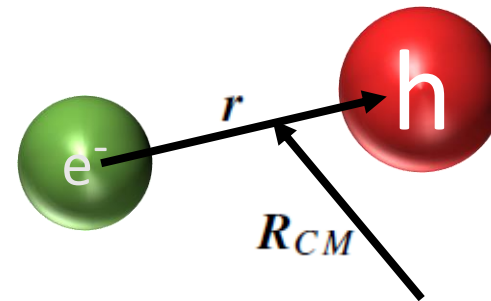
where e and h are the indices referring to the electron and hole, respectively.

Performing the standard procedure for the coordinate transformation to the center-of-mass and the relative motion coordinates:

D. Hughes, C. Eckart, Phys. Rev. 36, 694 (1930)

$$\mathbf{r} = \mathbf{r}_e - \mathbf{r}_h$$

$$\mathbf{R}_{CM} = (m_e \mathbf{r}_e + m_h \mathbf{r}_h) / (m_e + m_h)$$



Carl Jacobi (1804-1851) a German mathematician who made fundamental contributions to [elliptic functions](#), [dynamics](#), [differential equations](#), [determinants](#), and [number theory](#).

Jacobi Coordinate

$$\left[\frac{-\hbar^2}{2\mu} \nabla^2 + V(r) \right] \psi(\mathbf{r}) = E \psi(\mathbf{r}),$$

$\mu = m_e m_h / (m_e + m_h)$ the exciton reduced mass

In spherical coordinates the equation has the form

$$\frac{d^2}{dr^2}\psi(r, \theta, \varphi) + \frac{2}{r} \frac{d}{dr}\psi(r, \theta, \varphi) + \frac{1}{r^2} \left[\frac{1}{\sin \theta} \frac{d}{dr} \left(\sin \theta \frac{d}{d\varphi} \psi(r, \theta, \varphi) \right) + \frac{1}{\sin^2 \theta} \frac{d^2}{d\varphi^2} \psi(r, \theta, \varphi) \right] + \frac{2\mu}{h^2} [E - V(r)] \psi(r, \theta, \varphi)$$

The angular part of the Laplace operator in 3D configuration space

$$\hat{L} = \frac{1}{\sin \theta} \frac{d}{dr} \left(\sin \theta \frac{d}{d\varphi} \psi(r, \theta, \varphi) \right) + \frac{1}{\sin^2 \theta} \frac{d^2}{d\varphi^2} \psi(r, \theta, \varphi)$$

$$\hat{L}Y_{lm}(\theta, \varphi) = (l(l+1)Y_{lm}(\theta, \varphi))$$

Spherical harmonics are special functions defined on the surface of a **3D sphere**.



[Pierre-Simon Laplace, 1749–1827](#)

$$\frac{d^2}{dr^2}\psi(r) + \frac{2}{r} \frac{d}{dr}\psi(r) + \frac{l(l+1)}{r^2}\psi(r) + \frac{2\mu}{h^2} [E - V(r)] \psi(r) = 0$$

This equation describes the motion of one particle with reduced mass μ 3D configuration space

The question arises: For what type potential $V(r)$ can one solve the latter equation in the close analytical form?

Exact solution of two-body problem

If a two-body interaction $V(r)$ allows to the reduction of the radial Schrödinger equation to the form

$$\frac{d^2}{dr^2}\psi(r) + \frac{\tilde{\tau}(r)}{\sigma(r)} \frac{d}{dr}\psi(r) + \frac{\tilde{\sigma}(r)}{\sigma^2(r)}\psi(r) = 0,$$

where $\sigma(r)$ and $\tilde{\sigma}(r)$ are polynomials of degree at most 2, and $\tilde{\tau}(r)$ is a polynomial of degree at most 1.

$$\sigma(r) = a_0 + a_1 r + a_2 r^2$$

$$\tilde{\sigma}(r) = b_0 + b_1 r + b_2 r^2$$

$$\tilde{\tau}(r) = c_0 + c_1 r$$

The condition of the Nikiforov-Uvarov method

A. F. Nikiforov and V. B. Uvarov, Special Functions of Mathematical Physics, Birkhauser Basel, 1988

one can find the solution of the Schrödinger equation in the close analytical form in the framework of the Special Functions

Coulomb, Oscillator, Yukawa potentials

$$V(r) = D(1 - e^{-a(r-r_c)})^2 \quad \text{- Morse potential}$$

$$V(r) = \frac{g_1}{r^2} - \frac{g_2}{r} \quad \text{- Kratzer potential, *A. Kratzer, Z. Phys. 3, 289 (1920)*}$$

$$|V(r) = -\frac{\lambda(\lambda+1)}{2} \operatorname{sech}^2 r - \frac{\nu(\nu+1)}{2} \operatorname{csch}^2 r \quad \text{- Poschl-Teller potential}$$

$$V(r) = -\frac{\lambda(\lambda+1)}{2} \operatorname{sech}^2 r - g \tanh^2 r \quad \text{- Rosen-Morse potential}$$

Two-body problem in anisotropic materials

Within the effective mass approximation, the Hamiltonian for an interacting electron and hole with anisotropic effective mass, constrained to move in the plane of their respective monolayers, is given by

$$\hat{H}_0 = \frac{-\hbar^2}{2} \left(\frac{1}{m_e^x} \frac{\partial^2}{\partial x_e^2} + \frac{1}{m_e^y} \frac{\partial^2}{\partial y_e^2} + \frac{1}{m_h^x} \frac{\partial^2}{\partial x_h^2} + \frac{1}{m_h^y} \frac{\partial^2}{\partial y_h^2} \right) + V(\mathbf{r}_e - \mathbf{r}_h),$$

where the m_i^j , $j = x, y$, $i = e, h$ correspond to the effective mass of the electron or hole in the x or y direction, respectively.

For the separation of the relative motion of the electron-hole pair from its center-of-mass motion, one introduces variables for the center-of-mass of an electron-hole pair

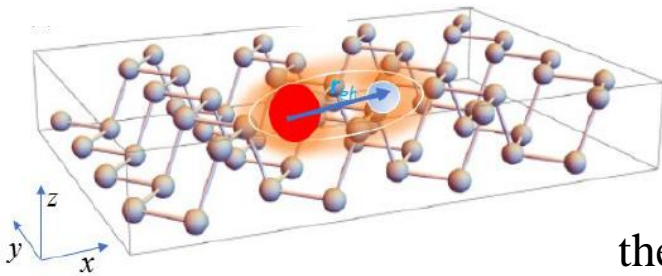
$$\mathbf{R} = (X, Y), X = (m_e^x x_e + m_h^x x_h) / (m_e^x + m_h^x), Y = (m_e^y y_e + m_h^y y_h) / (m_e^y + m_h^y)$$

$$\mathbf{r} = \mathbf{r}_e - \mathbf{r}_h \quad x = x_e - x_h, \quad y = y_e - y_h, \quad r^2 = x^2 + y^2$$

$$\left[-\frac{\hbar^2}{2\mu^x} \frac{\partial^2}{\partial x^2} - \frac{\hbar^2}{2\mu^y} \frac{\partial^2}{\partial y^2} + V(\mathbf{r}) \right] \psi(\mathbf{r}) = E \psi(\mathbf{r}),$$

where $\mu_x = \frac{m_e^x m_h^x}{m_e^x + m_h^x}$ and $\mu_y = \frac{m_e^y m_h^y}{m_e^y + m_h^y}$ are anisotropic reduced masses in x and y directions

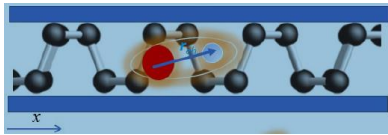
Thus, to find the eigenfunctions and eigenenergies of excitons one should solve two-dimensional equation even for the central potential



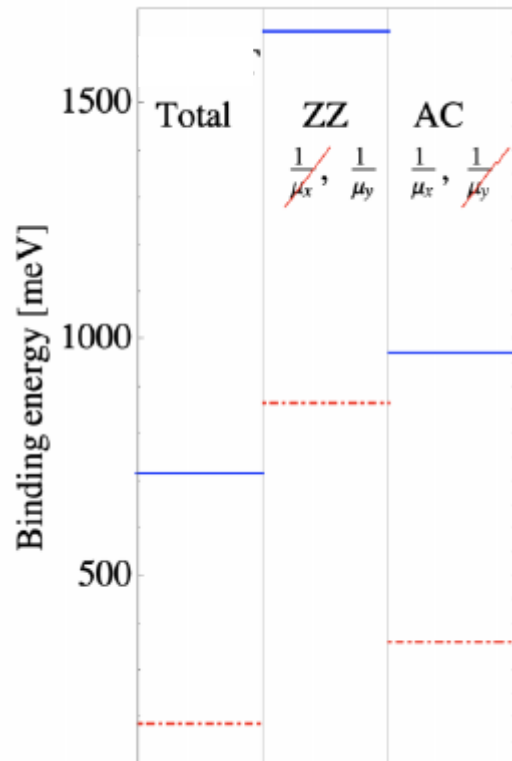
$$E = \left\langle -\frac{1}{2\mu_x} \frac{\partial^2}{\partial x^2} \right\rangle + \left\langle -\frac{1}{2\mu_y} \frac{\partial^2}{\partial y^2} \right\rangle + \langle V(x, y) \rangle$$

When $\mu_x > \mu_y$

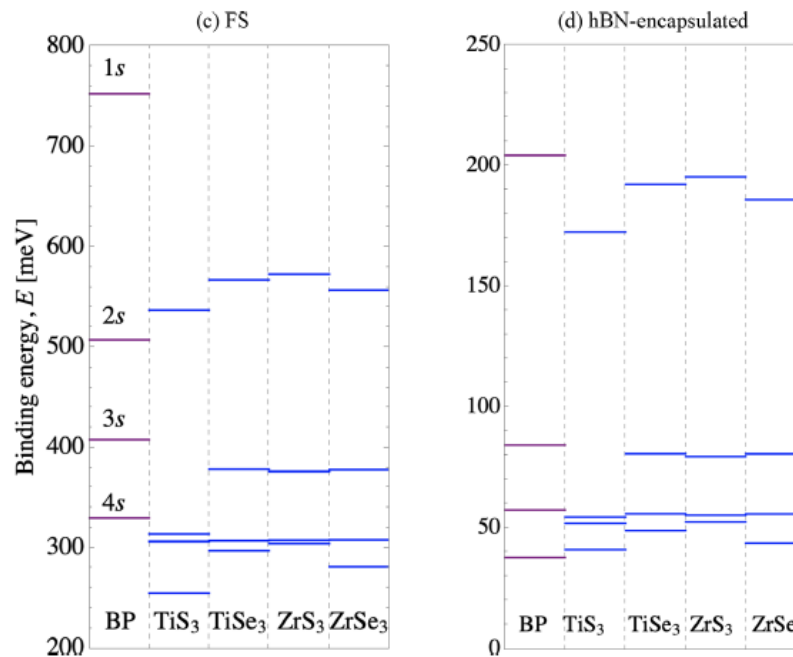
the contribution of the corresponding kinetic energy term is small that leads to larger binding energy. The relation $\mu_y > \mu_x$ leads to the opposite conclusion.



Phosphorene

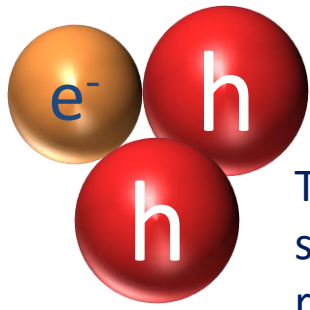


Transition Metal Trichalcogenide

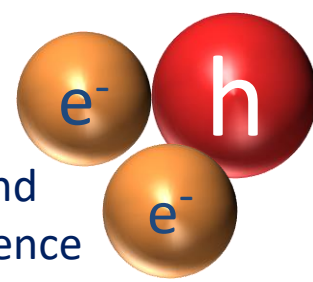


*Kezerashvili & Spiridonova,
Phys. Rev. Res. 4, 033016 (2022)*

*Kezerashvili & Spiridonova,
Phys. Rev. Res. 4, 013154 (2022)*



Trion



Trions in solid state physics are very similar to the few-body bound systems in atomic and nuclear physics but there is a major difference related to band effects:

- the effective masses of the electrons and holes smaller than the bare electron mass;
- screening effects, resulting from the host lattice, which make the Coulomb force much weaker than in atomic systems.

The Mott–Wannier trions in 2D and 3D semiconductors can be described by the solution of the three-body Schrödinger equation after modeling the crystal by effective electron and hole masses and a dielectric constant.

The nonrelativistic trion Hamiltonian is given by

$$H = -\frac{\hbar^2}{2} \sum_{i=1}^3 \frac{1}{m_i} \nabla_i^2 + \sum_{i < j}^3 V_{ij}(|\mathbf{r}_i - \mathbf{r}_j|).$$

For 2D semiconductors due to the space confinement the reduction of dimension leads to two-dimensional Laplace operators and the screened charge-charge interaction in 2D configuration space

Two Approaches

The low-energy effective two-band single-electron Hamiltonian in the form of a spinor with a gapped spectrum for TMDCs in the $k \cdot p$ approximation:

$$\hat{H}_s = at(\tau k_x \hat{\sigma}_x + k_y \hat{\sigma}_y) + \frac{\Delta}{2} \hat{\sigma}_z - \lambda \tau \frac{\hat{\sigma}_z - 1}{2} \hat{s}_z$$

The energy gap $\Delta = 1.6 -- 1.8 \text{ eV}$

The spin splitting $2\lambda = 0.1 -- 0.5 \text{ eV}$

Quasi-Relativistic approach

Berman, Kezerashvili, Zigler PRB 85, 035418 (2012)

Berman, Kezerashvili, Zigler PRA 87, 042513 (2013)

Berman and Kezerashvili, PRB 93, 245410 (2016)

A nonrelativistic approach within the framework of a potential model using effective mass approximation

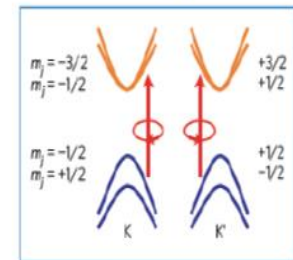
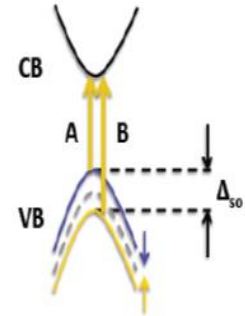
Berman, Kezerashvili, PRB 96, 094502 (2017)

$$\hat{H}_{ex} = -\frac{\hbar^2}{2m_e} \Delta_{\mathbf{r}_1} - \frac{\hbar^2}{2m_h} \Delta_{\mathbf{r}_2} + V(r)$$

Significant spin-orbit splitting in the valence band leads to the formation of TMDC layers two types of excitons:

Type A excitons are formed by spin-down holes from the valence band

Type B excitons are formed by spin-up holes from the valence band



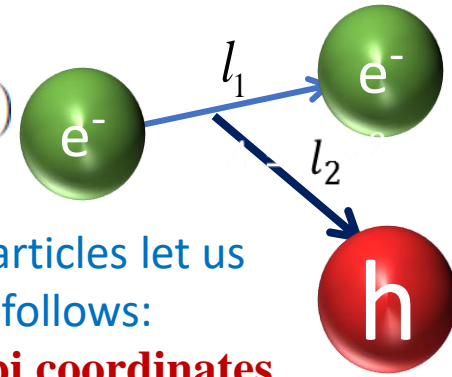
Mak, et al., Nat. Materials 12 (2013) 207

Theoretical Formalism

We study the X^- and X^+ trions

- in 3D bulk semiconductors within the Faddeev equation formalism
- 2D trions in TMDC semiconductors within the method of hyperspherical harmonics

$$\left[-\sum_{i=1}^3 \frac{\hbar^2}{2m_i} \nabla_i^2 + \sum_{i<j}^3 V_{ij}(x_i, x_j) \right] \Psi(\mathbf{r}_1, \mathbf{r}_2, \mathbf{r}_3) = E \Psi(\mathbf{r}_1, \mathbf{r}_2, \mathbf{r}_3)$$



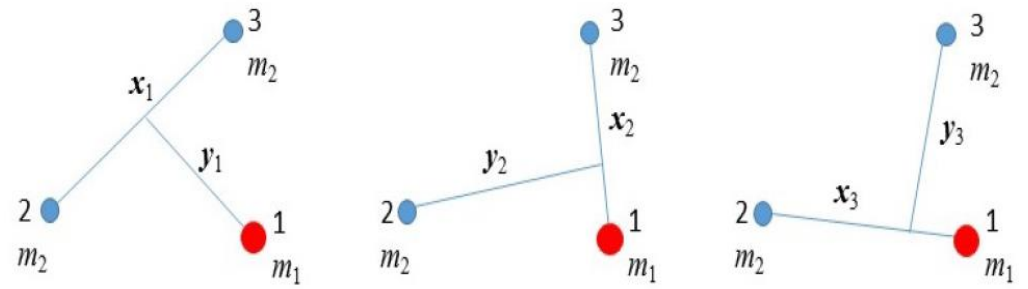
To separate out the center-of-mass and the relative motion of three particles let us introduce a set of mass-scaled Jacobi coordinates for the partition i as follows:

Mass-scaled Jacobi coordinates

$$\mathbf{x}_i = \sqrt{\frac{m_j m_k}{(m_j + m_k) \mu}} (\mathbf{r}_j - \mathbf{r}_k),$$

$$\mathbf{y}_i = \sqrt{\frac{m_i (m_j + m_k)}{(m_i + m_j + m_k) \mu}} \left(\frac{m_j \mathbf{r}_j + m_k \mathbf{r}_k}{m_j + m_k} - \mathbf{r}_i \right),$$

$$\mathbf{R} = \frac{m_1 \mathbf{r}_1 + m_2 \mathbf{r}_2 + m_3 \mathbf{r}_3}{M}, \quad M = m_1 + m_2 + m_3,$$



$$\left[-\frac{\hbar^2}{2\mu} (\nabla_{\mathbf{x}_i}^2 + \nabla_{\mathbf{y}_i}^2) + \sum_{i<j}^3 V_{ij}(x_i, x_j) - E \right] \Psi(\mathbf{x}_i, \mathbf{y}_i) = 0$$

The Schrodinger equation for the relative motion of the three-body system in 3D or 2D space

Faddeev Formalism



G.V. Skorniakov, K.A. Ter-Martirosian, ZhETF **31**, 775 (1957);

L.D. Faddeev, ZhETF **39**, 1459 (1961); [Sov. Phys. JETP **12**, 1014 (1961)]

L.D. Faddeev, Mathematical problems of the quantum theory of scattering for a system of three particles. Proc. Math. Inst. Acad. Sciences USSR **69**, 1–122 (1963)

The Faddeev reformulation of the three-body Schrodinger equation amounts to converting this equation into a set of multiple-scattering equations in which the pair interaction is represented by full subsystem transition amplitudes.

$$T = T_1 + T_2 + T_3$$

$$|\psi^+\rangle = |\psi^{(1)}\rangle + |\psi^{(2)}\rangle + |\psi^{(3)}\rangle,$$

with $\psi^{(i)}$ satisfying

$$|\psi^{(i)}\rangle = |\phi_\rho^{(i)}\rangle \delta_{t_1} + \sum_{j \neq i} G_0 t_j |\psi^{(j)}\rangle$$

G_0 is the free Green's operator and t_i is the two-particle transition operator acting in the three-particle space.

Ludvig Dmitrievich Faddeev
(1934 –2017) was a Soviet
and Russian mathematical
physicist

In general, Faddeev equations need as input a **potential** that describes the interaction between two individual particles. It is also possible to introduce a term in the equation in order to take also three-body forces into account.

L.D. Faddeev, S.P. Merkuriev, *Quantum Scattering Theory for Several Particle Systems* (Nauka, Moscow, 1985)

L.D. Faddeev, S.P. Merkuriev, *Quantum Scattering Theory for Several Particle Systems* (Kluwer Academic, Dordrecht, 1993)

Trion on in 2D and 3D materials

Initial work on trion binding energies in TMDCs employed:

- variational wave functions
- the time-dependent density-matrix functional theory
- the fractional dimensional space approach
- the stochastic variational method with explicitly correlated Gaussian basis
- method of hyperspherical harmonics
- quantum Monte Carlo methods, such as the diffusion Monte Carlo and the path integral Monte Carlo

[T.C. Berkelbach, M.S. Hybertsen, D.R. Reichman, Phys. Rev. B 88 \(2013\) 045318.](#)

[A. Thilagam, J. Appl. Phys. 116 \(2014\) 053523.](#)

[A. Ramirez-Torres, V. Turkowski, T.S. Rahman, Phys. Rev. B 90 \(2014\) 085419.](#)

[I. Kylänpää, H.-P. Komsa, Phys. Rev. B 92 \(2015\) 205418.](#)

[K.A. Velizhanin, A. Saxena, Phys. Rev. B 92 \(2015\) 195305.](#)

[B. Ganchev, N. Drummond, I. Aleiner, V. Fal'ko, Phys. Rev. Lett. 114 \(2015\) 107401.](#)

[M.Z. Mayers, T.C. Berkelbach, M.S. Hybertsen, D.R. Reichman, Phys. Rev. B 92 \(2015\) 161404.](#)

[D.K. Zhang, D.W. Kidd, K. Varga, Phys. Rev. B 93 \(2016\) 125423.](#)

[G.G. Spink, P. López Rós, N.D. Drummond, R.J. Needs, Phys. Rev. B 94 \(2016\) 041410.](#)

[R.Ya. Kezerashvili, Sh.M. Tsiklauri, Few-Body Syst. 58 \(2017\) 18.](#)

[M. Szytniszewski, E. Mostaani, N.D. Drummond, V.I. Falko, Phys. Rev. B 95 \(2017\) 081301\(R\).](#)

[R. Maezono, M. Szytniszewski, C.H. Price, R. Maezono, M. Danovich, R.J. Hunt,](#)

[arXiv:1706.04688v1 \[cond-mat.mes-hall\], PHYS Rev. B 2007.](#)

Kezerashvili, Few-Body Syst (2019) 60:52

See review:

Though much progress has been made, intrinsic excitonic states of 2D and 3D trions are still highly debated in theory, particularly related to the binding energies for negatively and positively charged trions

3D Trions within Faddeev Formalism

The Faddeev equations in 3D conguration space can be written in the form of system of second order differential equations *Faddeev, Merkuriev., 1993.*

$$\begin{aligned}(H_0 + V_{AA} - E)U &= -V_{AA}(W - PW), \\ (H_0 + V_{AB} - E)W &= -V_{AB}(U - PW).\end{aligned}$$

where P is the permutation operator for two identical particles.

$$\Psi = U + W \pm PW$$

Wave function is asymmetric with respect to the permutation operator P

$$\Psi: P\Psi = P(U + W - PW) = -U + PW - W = -\Psi$$

The Hamiltonian H_0 is the operator of kinetic energy written in terms of corresponding Jacobi coordinates, while V_{AA} and V_{AB} are the potentials of the pairwise interactions between the particles.

Binding Energy of Trions in Bulk Semiconductors

Material	m_e/m_0	m_h/m_0	ϵ	X	X^-	X^+
InN	0.11	1.63	7.5 [3]	24.88	3.6	—
GaAs	0.067	0.51	12.9	4.83	0.5	Unbound
ZnSe	0.16	0.75	8.6	24.2	2.1	Unbound
GaN	0.2	0.82	8.9	27.57	2.1	Unbound
CdTe	0.096	0.35	10.16	9.91	0.6	≈ 0.1
MoS ₂	0.45	0.45	10.7 [5, 4]	26.7	~ 0.1	—
MoS ₂	0.590	0.838	10.6 [1, 2]	41.85	0.6	Unbound
MoSe ₂	0.521	0.973	11.35 [1, 2]	35.77	0.2	Unbound
WS ₂	0.569	0.832	9.25 [1, 2]	53.63	1.3	Unbound
WSe ₂	0.489	0.997	10.61 [1, 2]	39.58	0.4	—

Positively charged trion in 3D bulk materials is unbound for all set of parameters

The X^- and X^+ trions and neutral exciton X binding energies in meV for different bulk semiconductors.

Dielectric constant is the main factor that effects X^- trion binding energy.

Origin of the difference of binding energies of trions

To analyze and understand the origin of the difference of binding energies for the X^- and X^+ trions one can write the Schrödinger equation for the trion in the system of reference relative to the non-identical particle:

$$\left(-\frac{\hbar^2}{2\mu}\nabla_{r_{A_1}}^2 - \frac{\hbar^2}{2\mu}\nabla_{r_{A_2}}^2 - \frac{\hbar^2}{m_B}\nabla_{r_{A_1}}\nabla_{r_{A_2}} + V_{AB}(r_{A_1}) + V_{AB}(r_{A_2}) - V_{AA}(r_{A_1} - r_{A_2}) - E_3\right)\Psi(r_{A_1}, r_{A_2}, r_{A_1} - r_{A_2}) = 0,$$

$$T_{mp} = -\frac{\hbar^2}{m_B}\nabla_{r_{A_1}}\nabla_{r_{A_2}} \text{ the mass-polarization term}$$

In the case $m_B < m_A$ the contribution of the MPT can be of the same order as the contribution of the other two differential operators due to the comparable mass factors of these operators, which can be expressed as $1/m_B$. In the case $m_B > m_A$ the contribution of this term has the factor $1/m_B$, while the mass factors of other differential operators are of the order of $1/m_A$.

If the MPT and the interaction $V_{AA} \equiv V_{AA}(r_{A1}, r_{A2}, r_{A1}-r_{A2})$ between two identical particles are neglected one obtains:

$$\left(-\frac{\hbar^2}{2\mu}\nabla_{r_{A1}}^2 - \frac{\hbar^2}{2\mu}\nabla_{r_{A2}}^2 + V_{AB}(r_{A1}) + V_{AB}(r_{A2}) - E_3(T_{mp} = 0, V_{AA} = 0)\right)\Psi(r_{A1}, r_{A2}) = 0$$

The total wave function can be factorized that leads to the trivial solution:

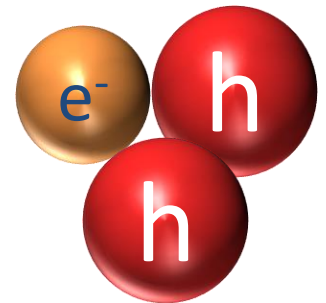
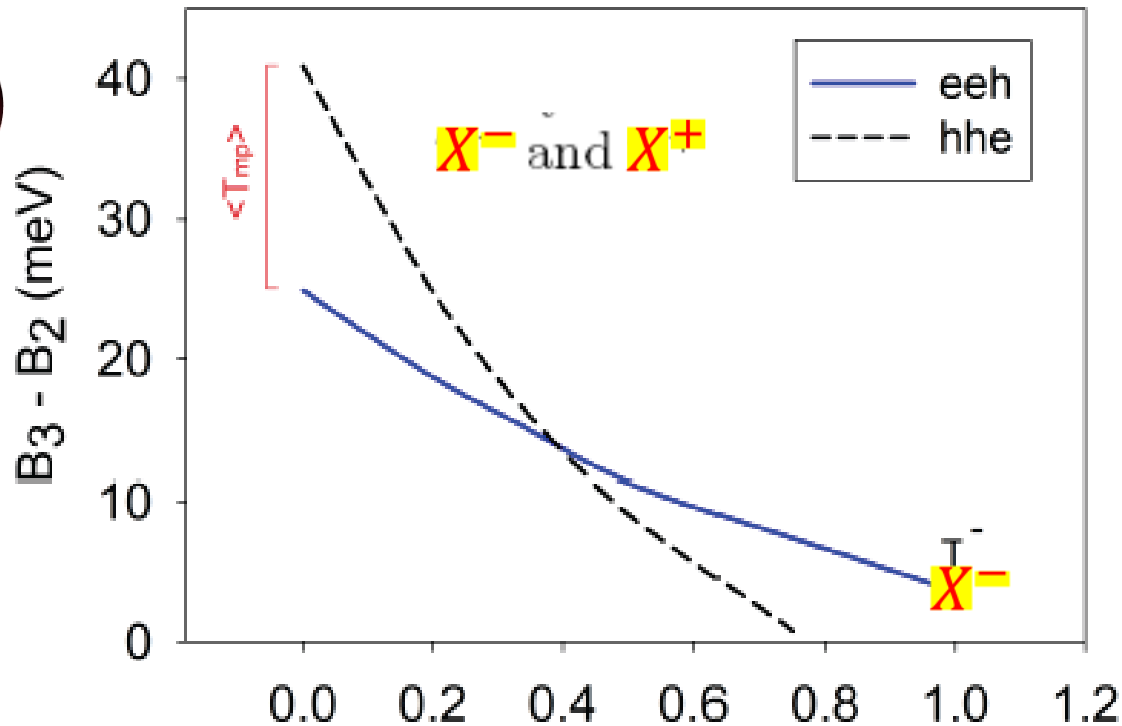
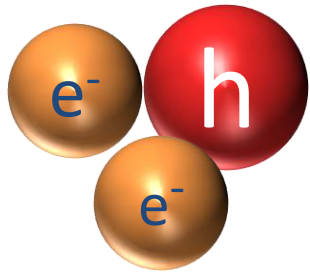
$$E_3(T_{mp} = 0, V_{AA} = 0) = 2E_2,$$

where E_2 is the ground state energy of two-body subsystem AB . Within our consideration the bound AB pair is the exciton.

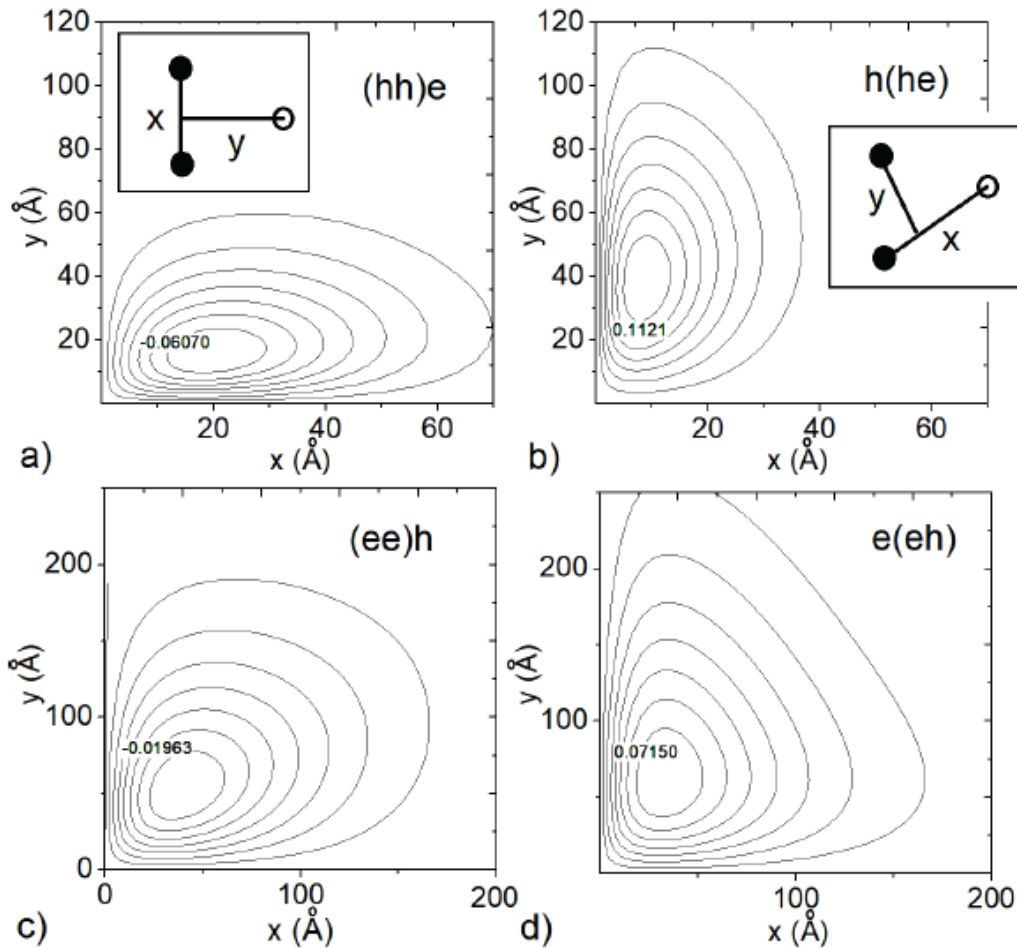
$$E_3 = -\langle T_1 \rangle - \langle T_2 \rangle + \langle V_{AB} \rangle + \langle V_{AB} \rangle - \langle T_{mp} \rangle + \alpha \langle V_{AA} \rangle$$

The origin of binding energies difference for X^- and X^+ trions

Let's introduce the interaction between two identical particles as $\alpha \langle V_{AA} \rangle$, where the parameter α controls the strength of this interaction.



Eigen functions for *eeh* and *hhe* systems



The negative triion has more extended distribution within about 300×400 Å, than less extended distribution within 100×100 Å for the positive triion.

Thus,

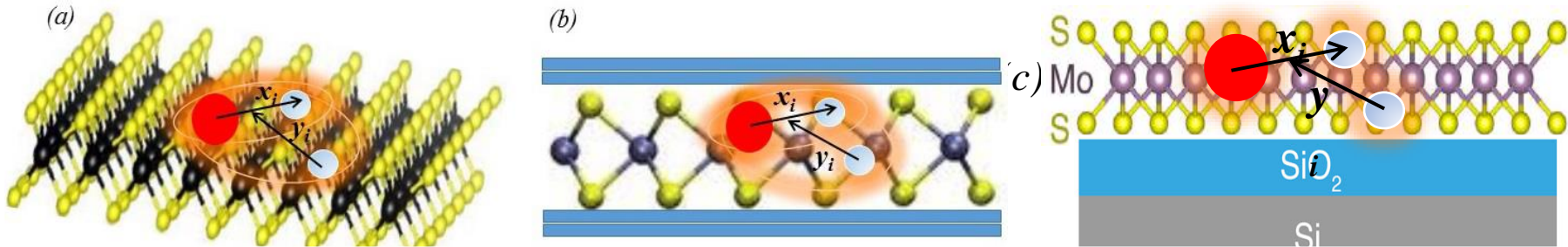
two heavy holes are located more closer to each other in X^+ than two electrons in X^-

Conclusion

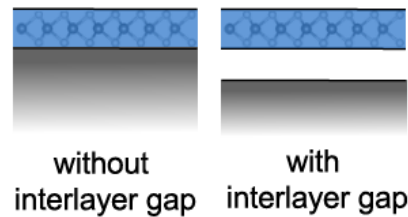
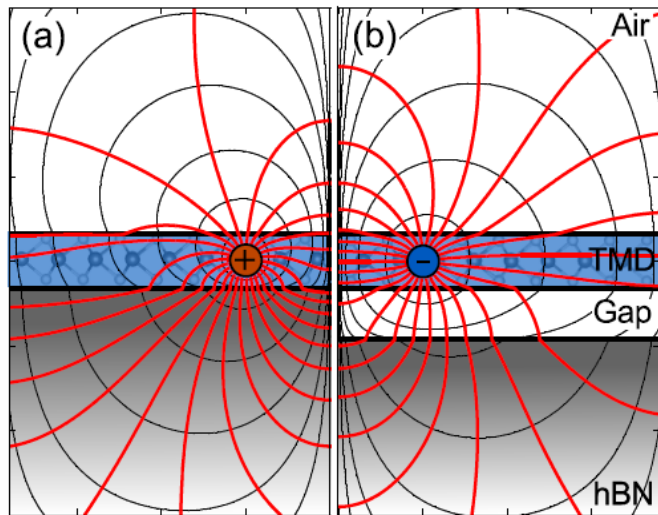
The hole-hole Coulomb repulsion is stronger in X^+ than the electron-electron repulsion in X^- due to more close localization of the two holes

The contour plots of the Faddeev components U and W for *eeh* and *hhe* systems

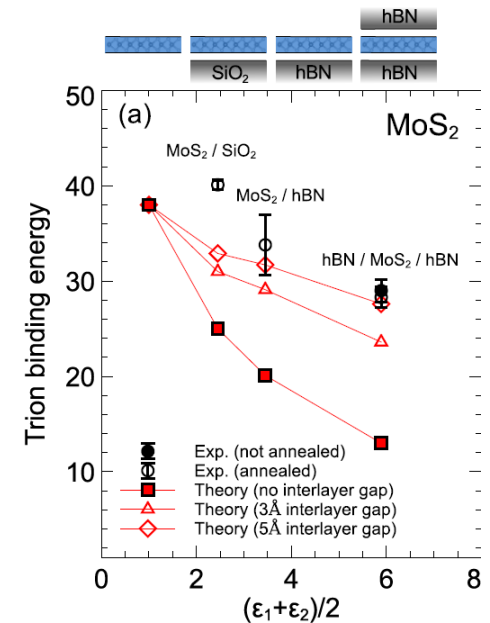
2D Trions



Schematic representation of the trion in (a) freestanding, (b) encapsulated and (c) supported TMDC monolayer. x_i and y_i are Jacobi coordinates for the partition i .

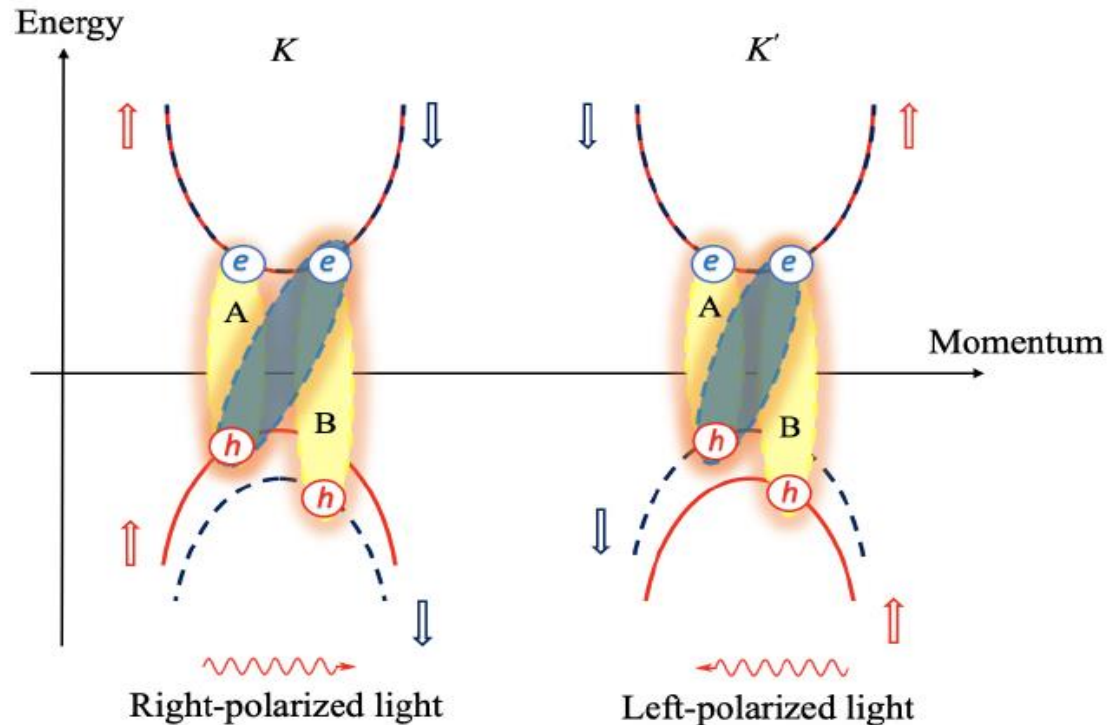


M. Florian, et al. Nano Lett. 18, 2725 (2018).



Schematic representation of a supported monolayer with (a) an ideal plane boundary and (b) a realistic interface with a finite interlayer gap.

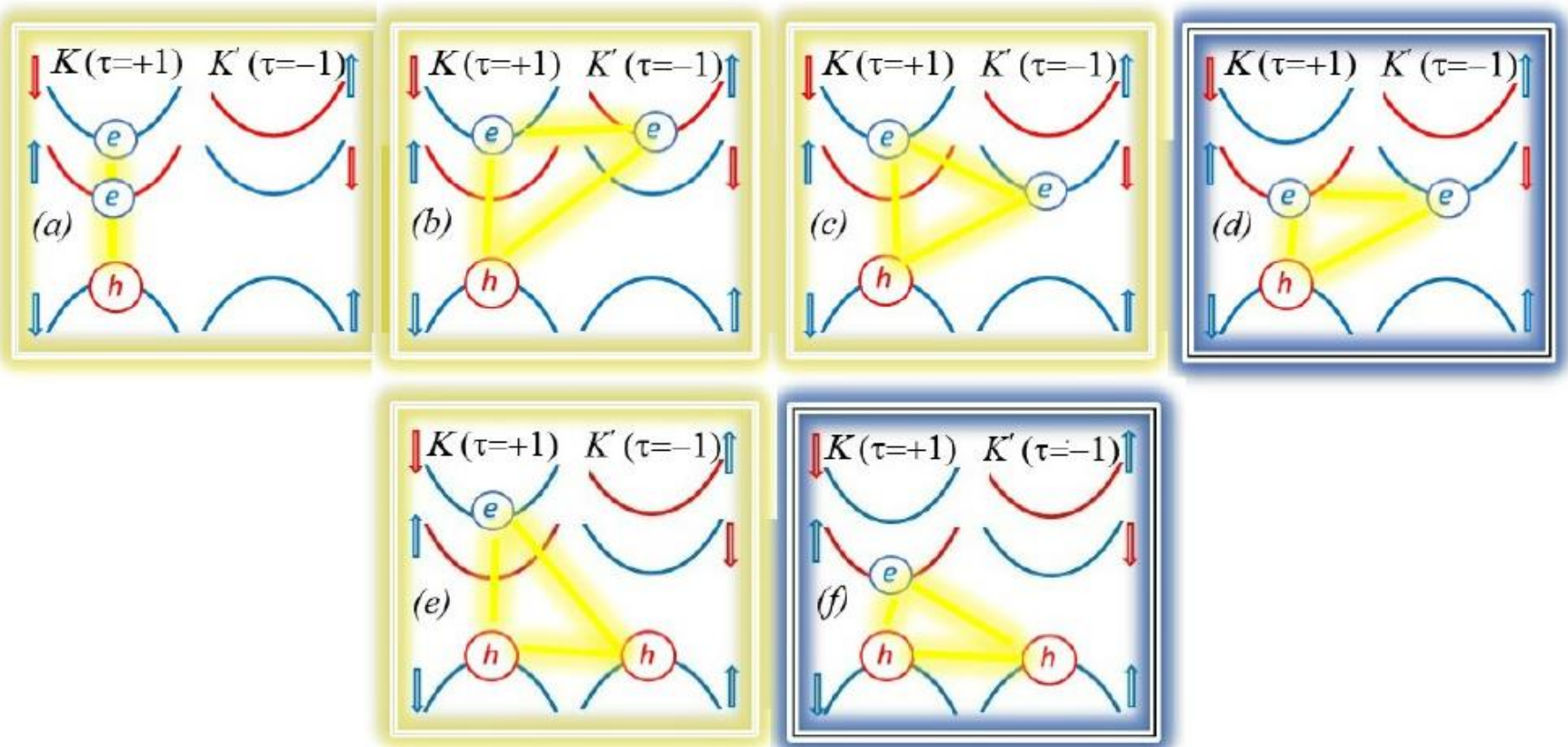
Bright and dark excitons



The schematic band structure and electronic dispersions in the TMDC monolayer for bright and dark excitons in the K and K' valleys. Spin-up and spin-down bands are denoted by red and blue curves, respectively. The yellow shadowed ovals are the bright excitons and correspond to the lowest optically induced transition between the bands of the same spin at the K and K' point. The dark shadowed oval is the spin-forbidden dark exciton (the second one is not shown). The units of the vertical and horizontal axes are arbitrary. At point K the right circular polarized light couples to both A and B exciton transitions. At point K' the left circular polarized light couples to A and B excitons.

Intravalley and intervalley 2D Trions

Schematic illustration of WSe_2 low-energy band structure and the spin-valley configurations of the constituent charge carriers. It is shown the topmost spin-subband for the valence band and the lower and upper spin-orbit splitting conduction band. Light and dark rectangles indicate the bright and dark trions, respectively. (a), (b), (c), and (d) correspond to X^- trions. (e) and (f) correspond to X^+ trions. Lines indicate interaction between three charged particles.

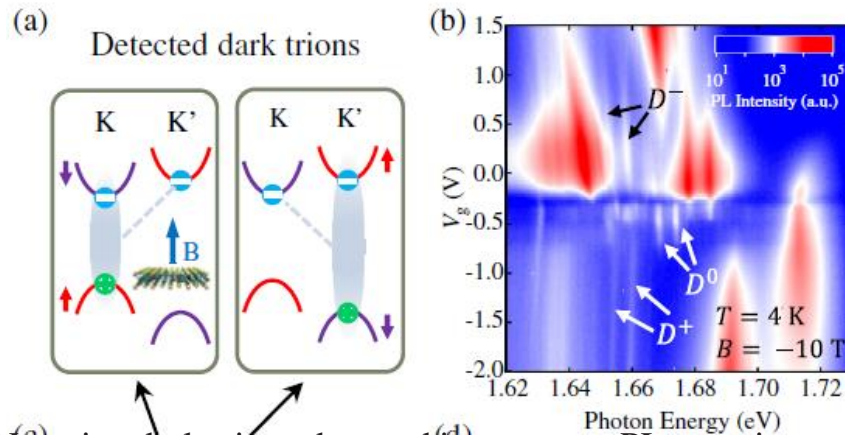
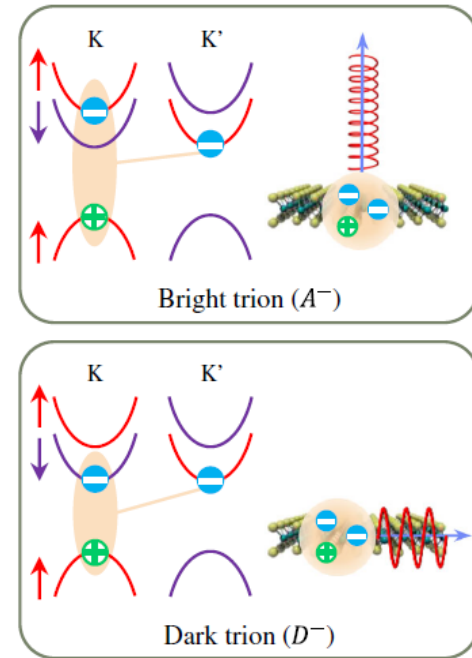


Intravalley Bright and Dark 2D Trions

E. Liu, PRL 123, 027401 (2019)

Monolayer WSe₂ is an intriguing material to explore dark exciton physics. The dark trions can be tuned continuously between negative and positive trions with electrostatic gating. The dark trion binding energies are **14–16 meV**.

This is slightly lower than the bright trion binding energies (**21–35 meV**). The dark trion lifetime (**~1.3 ns**) is two orders of magnitude longer than the bright trion lifetime (**~10 ps**)



(a) Negative dark trions detected in magneto-PL experiment.
 (b) Dark excitons and trions in monolayer WSe₂ are split into two peaks, whereas bright excitons and trions are not.

FIG. 1. Intervalley bright and dark trions in monolayer WSe₂. The red (blue) lines denote bands with up (down) electron spin. The shaded ellipses denote excitons involved in recombination. The bright excitons and trions emit circularly polarized light in the out-of-plane direction. The dark excitons and trions emit vertically polarized light in the in-plane direction.

Dark trions have a distinct spin configuration from that of bright trions.
Bright trions involve a spin singlet exciton, dark trions involve a spin-triplet exciton

2D Trions within Hyperspherical Harmonics Formalism

The Schrodinger equation for the relative motion of the three-body system
in 2D space

$$\left[-\frac{\hbar^2}{2\mu} (\nabla_{x_i}^2 + \nabla_{y_i}^2) + \sum_{i < j}^3 V_{ij}(x_i, x_j) - E \right] \Psi(\mathbf{x}_i, \mathbf{y}_i) = 0$$

To obtain a solution of the Schrodinger equation for the trion we employ
hyperspherical coordinates in 4D configuration space.

Let us introduce in 4D space the hyperradius $\rho = \sqrt{x_i^2 + y_i^2}$ and a set of three angles $\Omega_i \equiv (\alpha_i, \varphi_{x_i}, \varphi_{y_i})$, where φ_{x_i} and φ_{y_i} are the polar angles for the Jacobi vectors \mathbf{x}_i and \mathbf{y}_j , respectively, and α_i is an angle defined as $x_i = \rho \cos \alpha_i$, $y_i = \rho \sin \alpha_i$. After the transformation from the Jacobi coordinates \mathbf{x}_i and \mathbf{y}_i to the hyperspherical coordinates ρ, Ω_i , Schrodinger equation can be rewritten as

$$\left[-\frac{\hbar^2}{2\mu} \left(\frac{\partial^2}{\partial \rho^2} + \frac{3}{\rho} \frac{\partial}{\partial \rho} - \frac{\hat{K}^2(\Omega_i)}{\rho^2} \right) + \sum_{i > j}^3 V_{ij}(|\mathbf{r}_i - \mathbf{r}_j|) - E \right] \Psi(\rho, \Omega_i) = 0$$

$$\hat{K}^2(\Omega_i) = -\frac{d^2}{d\alpha_i^2} - 2 \cot 2\alpha_i \frac{d}{d\alpha_i} + \frac{\hat{l}^2(\varphi_{x_i})}{\cos \alpha_i} + \frac{\hat{l}^2(\varphi_{y_i})}{\sin \alpha_i},$$

$$\hat{l}(\varphi_{x_i}) = -i \frac{d}{d\varphi_{x_i}}, \quad \hat{l}(\varphi_{y_i}) = -i \frac{d}{d\varphi_{y_i}}, \quad \Omega_i \equiv (\alpha_i, \hat{\mathbf{x}}_i, \hat{\mathbf{y}}_i)$$

$$\hat{K}^2(\Omega_i) \Phi_K^{l_x m_x l_y m_y}(\Omega) = K(K+2) \Phi_K^{l_x m_x l_y m_y}(\Omega)$$

$$\Phi_{K\lambda}^{LM}(\Omega) = \sum_{m_x m_y} \langle l_x m_x l_y m_y | LM \rangle \Phi_K^{l_x m_x l_y m_y}(\Omega),$$

where we use the short-hand notation $\lambda \equiv \{l_x, l_y\}$, and $\langle l_x m_x l_y m_y | LM \rangle$ are the Clebsch–Gordan coefficients

$$\Psi(\rho, \Omega_i) = \rho^{-3/2} \sum_{K\lambda} u_{K\lambda}^L(\rho) \Phi_{K\lambda}^{LM}(\Omega) \chi_s \phi_\tau.$$

- *Jibuti & Kezerashvili, Nuclear Physics A438 (1984) 573;*
- *Jibuti & Kezerashvili, Nuclear Physics A437 (1985) 687*

$u_{K\lambda}^L(\rho)$ are the hyperradial functions, where L is the total orbital angular momentum of the trion

$$\left[\frac{d^2}{d\rho^2} - \frac{(K+1)^2 - 1/4}{\rho^2} + \kappa^2 \right] u_{K\lambda}^L(\rho) = \frac{2\mu}{\hbar^2} \sum_{K'\lambda'} \mathcal{W}_{K\lambda K'\lambda'}^L(\rho) u_{K'\lambda'}^L(\rho)$$

$$\mathcal{W}_{K\lambda K'\lambda'}(\rho) = \frac{\pi k}{2\epsilon\rho_0} \int \Phi_{K\lambda}^{L*}(\Omega_i) \sum_{i<j}^3 q_i q_j \left[H_0\left(\frac{x_j}{b_j\rho_0}\right) - Y_0\left(\frac{x_j}{b_j\rho_0}\right) \right] \Phi_{K'\lambda'}^L(\Omega_i) d\Omega_i$$

$$\Phi_{K\lambda_i}^L(\Omega_i) = \sum_{\lambda_k} \langle \lambda_k | \lambda_i \rangle_{KL} \Phi_{K\lambda_k}^L(\Omega_k),$$

where $\langle \lambda_k | \lambda_i \rangle_{KL} \equiv \langle l_{x_k} l_{y_k} | l_{x_i} l_{y_i} \rangle_{KL}$ are Reynal-Revai coefficients.

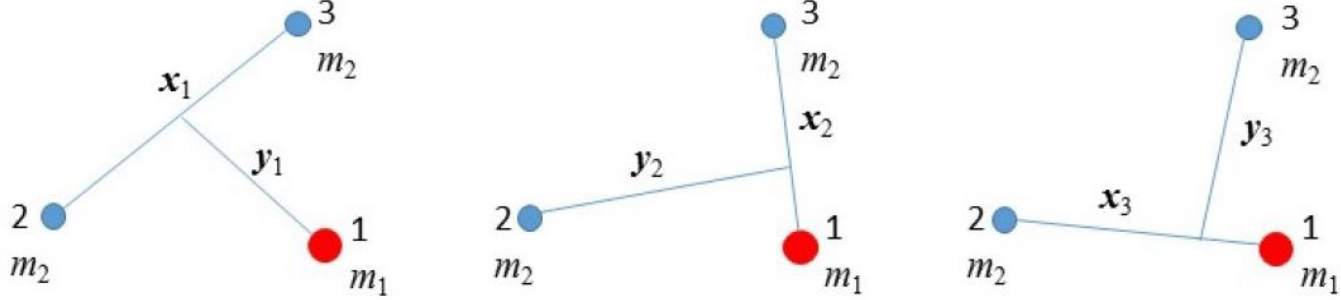


FIG. 1: (Color online) The partition trees of Jacobi coordinates for X^- trion.

By using the Reynal-Revai unitary transformation

$$W_{KK' \lambda\lambda'}^L(\rho) = \left(\mathcal{K}_{K\lambda K'\lambda'}^{(1)} - \sum_{\lambda_k \lambda'_k} \langle \lambda_k | \lambda_i \rangle_{KL} \langle \lambda'_k | \lambda_i \rangle_{K'L} \mathcal{K}_{K\lambda K'\lambda'}^{(2)} - \sum_{\lambda_j \lambda'_j} \langle \lambda_j | \lambda_i \rangle_{KL} \langle \lambda'_j | \lambda_i \rangle_{K'L} \mathcal{K}_{K\lambda K'\lambda'}^{(3)} \right)$$

$$\mathcal{K}_{K\lambda K'\lambda'}^{(i)} = \frac{\pi k e^2}{2\epsilon \rho_0} \int \Phi_{K\lambda}^{L*}(\Omega_i) \left[H_0\left(\frac{\rho \cos \alpha_i}{b_i \rho_0}\right) - Y_0\left(\frac{\rho \cos \alpha_i}{b_i \rho_0}\right) \right] \Phi_{K'\lambda'}^L(\Omega_i) \cos \alpha_i \sin \alpha_i d\alpha_i d\varphi_{x_i} d\varphi_{y_i}, \quad i = 1, 2, 3.$$

Using the matrix elements of the effective potential energies given above, one can solve the coupled differential equations numerically.

Analytical Solutions

Long-range limit: $r \gg \rho_0$ $V_{ij}(r) = \frac{kq_i q_j}{\epsilon r}$ Coulomb Potential

$$\left[\frac{d^2}{d\rho^2} - \frac{(K+1)^2 - 1/4}{\rho^2} + \kappa^2 \right] u_{K\lambda}^L(\rho) = \frac{2\mu}{\hbar^2} \sum_{K'\lambda'} \mathcal{W}_{K\lambda K'\lambda'}^L(\rho) u_{K'\lambda'}^L(\rho)$$

The set of coupled differential equations for the hyperradial functions $u^L(\rho)$

In the diagonal approximation $K = K', \lambda = \lambda'$

$$\mathcal{W}_{K\lambda K\lambda}^L(\rho) = k \int \Phi_{K\lambda}^{L*}(\Omega_i) \left(\frac{b_1}{x_1} - \frac{b_2}{x_2} - \frac{b_3}{x_3} \right) \Phi_{K\lambda}^L(\Omega_i) d\Omega_i$$

All integrals can be evaluated in a closed analytic form, and we have the equation with the Coulomb-like potential

$$\left[\frac{d^2}{d\rho^2} - \frac{(K+1)^2 - 1/4}{\rho^2} + \kappa^2 \right] u_{K\lambda}^L(\rho) = \frac{2\mu}{\hbar^2} \frac{\mathcal{G}_{K\lambda K\lambda}^L}{\rho} u_{K\lambda}^L(\rho)$$

$$E = -\frac{\mu}{\hbar^2} \frac{(\mathcal{G}_{K\lambda K\lambda}^L)^2}{2(N+K+3/2)^2}$$

$$u_K(\rho) = C_K \rho^{K+3/2} \exp(-\kappa\rho) L_N^{2K+2}(2\kappa\rho)$$

where $N = 1, 2, \dots$, L_N^{2K+2} is a Laguerre polynomial, C_K is a normalization constant

Analytical Solutions

Short-range limit: $r \ll \rho_0$ $V_{ij}(r) = \frac{kq_i q_j}{\epsilon \rho_0} \left[\ln \left(\frac{r}{2\rho_0} \right) + \gamma \right]$

Logarithmic Potential

The set of coupled differential equations for the hyperradial functions $u^L(\rho)$ in the diagonal approximation $K = K', \lambda = \lambda'$ has the form

$$\left[\frac{d^2}{d\rho^2} + \left(\alpha - \beta \ln \varrho - \frac{\gamma}{\varrho^2} \right) \right] u_{K\lambda}^L(\rho) = 0$$

$$\alpha = \kappa^2(2\mu B/\hbar^2) - \frac{2\mu}{\hbar^2} \left(-\frac{ke^2}{\epsilon \rho_0} \ln \rho_0 + B_{123} + \mathcal{J}_{K\lambda K\lambda} \right), \quad \beta = \frac{2\mu}{\hbar^2} \frac{ke^2}{\epsilon \rho_0}, \quad \gamma = (K+1)^2 - 1/4.$$

We found the analytical solution of this equation by rescaling the variable ρ and introducing a new function that allows to reduce it to the known Weber's equation [Weber, Math. Ann., 1, 1 \(1869\)](#).

We introduce new variable z as

$$V(z) = -z\beta e^{2\alpha/\beta + 2z}$$

$$\rho = e^{z-\alpha/\beta}, \quad (-\infty < z < \infty) \Rightarrow u_{K\lambda} = e^{z-\alpha/\beta} \Phi(z) \Rightarrow \frac{d^2 \Phi(z)}{dz^2} + [-\Delta^2 + V(z)] \Phi(z) = 0$$

$$E = -\frac{ke^2}{\epsilon \rho_0} \ln \rho_0 + B_{123} + \mathcal{J}_{K\lambda K\lambda} + \frac{ke^2}{\epsilon \rho_0} \left\{ 1 + \ln \left[\frac{[n + 1/2 + \sqrt{(n + 1/2)^2 + \Delta^2/16}]^2}{\frac{2\mu}{\hbar^2} \frac{ke^2}{\epsilon \rho_0}} \right] \right\}, \quad n = 0, 1, 2, \dots$$

$$\Phi = D_n(w) = 2^{(n-1)/2} e^{-w^2/4} F\left(\frac{1-n}{2}, \frac{3}{2}, \frac{w^2}{2}\right), \quad F\left(\frac{1-n}{2}, \frac{3}{2}, \frac{w^2}{2}\right) \text{ is a confluent hypergeometrical function.}$$

Result in Short- and Long-range limit Approximations

X^- trion binding energies in meV in the short $r \ll \rho_0$ and long $r \gg \rho_0$ range limits.

	Theory, $r \ll \rho$		Theory, $r \gg \rho$		Experiment
	This work	[37]	This work		
MoS ₂	27.2	29 – 31	21.1		18 ± 1.5 [5], 30, 32 [11]
MoSe ₂	25.3	29 – 31	21.3		30 [6, 9]
WS ₂	29.1	28 – 30	22.5		30 [15], 45 [12]
WSe ₂	27.5	28 – 30	21.8		30 [7, 8]

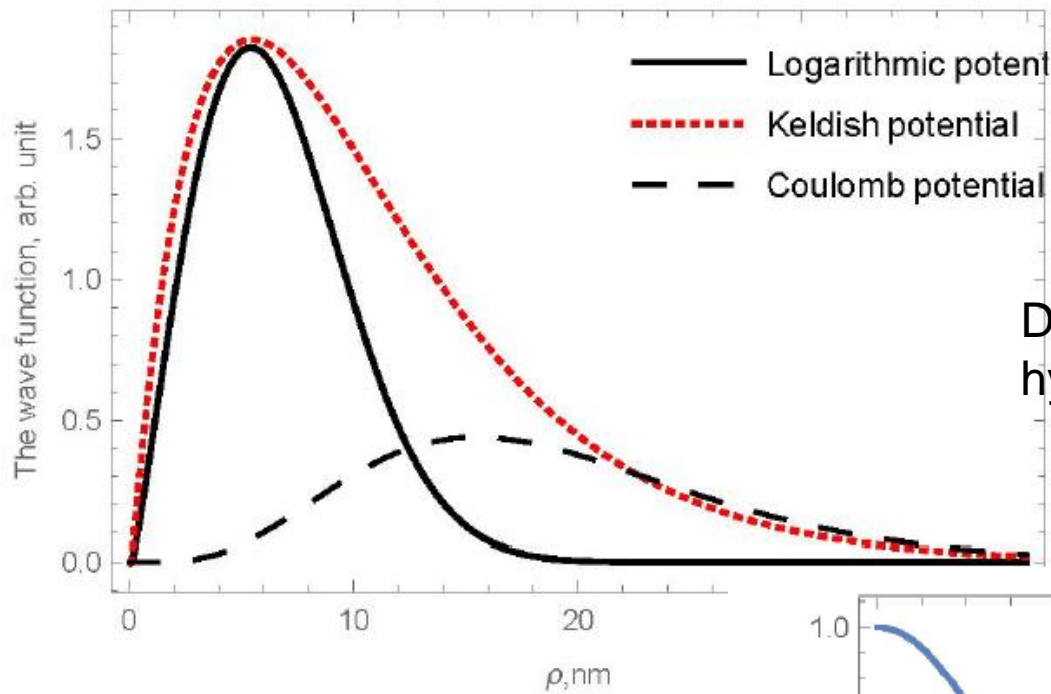
[37] B. Ganchev, N. Drummond, I. Aleiner, and V. Fal'ko, *Phys. Rev. Lett.* 114, 107401 (2015).

Calculations performed in the diagonal approximation, when $K = 0$.

	m_e/m_0	m_h/m_0	$\rho_0, \text{Å}^0$
MoS ₂	0.350	0.428	38.62[65]
MoSe ₂	0.38	0.44	51.71[22]
WS ₂	0.27	0.32	37.89[22]
WSe ₂	0.29	0.34	45.11[22]

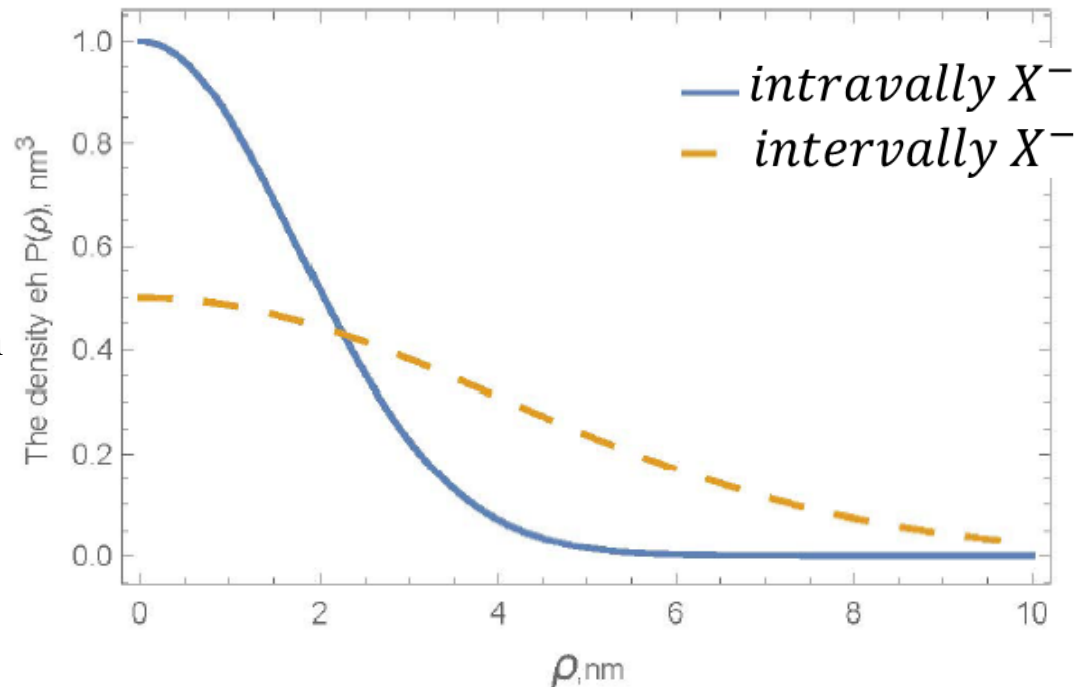
	Short-range limit: $r \ll \rho$			Long-range limit: $r \gg \rho_0$		
	Freestanding	Supported	Encapsulated	Freestanding	Supported	Encapsulated
MoS ₂	27.2	23.1	22.9	21.1	16.1	15.8
MoSe ₂	25.3	17.2	16.8	21.3	16.3	16.0
WS ₂	29.1	21.2	20.3	22.5	17.2	16.5
WSe ₂	27.5	16.4	15.1	21.8	16.4	16.1

Calculations performed in the diagonal approximation for intravalley X^- , when $K = 0$ for freestanding, supported by SiO₂ and hBN encapsulated TMDC monolayers



Dependence radial wave function on hyperradius for different potentials

Density distribution for an intravalley and intervalley negatively charged trion



Analytical Solutions

$$\text{Short-range limit: } r \ll \rho_0 \quad V_{ij}(r) = \frac{kq_i q_j}{\epsilon \rho_0} \left[\ln \left(\frac{r}{2\rho_0} \right) + \gamma \right]$$

Logarithmic Potential

The set of coupled differential equations for the hyperradial functions $u^L(\rho)$ in the diagonal approximation $K = K', \lambda = \lambda'$ has the form

$$\left[\frac{d^2}{d\rho^2} + \left(\alpha - \beta \ln \rho - \frac{\gamma}{\rho^2} \right) \right] u_{K\lambda}^L(\rho) = 0$$

$$\alpha = \kappa^2(2\mu B/\hbar^2) - \frac{2\mu}{\hbar^2} \left(-\frac{ke^2}{\epsilon \rho_0} \ln \rho_0 + B_{123} + \mathcal{J}_{K\lambda K\lambda} \right), \quad \beta = \frac{2\mu}{\hbar^2} \frac{ke^2}{\epsilon \rho_0}, \quad \gamma = (K+1)^2 - 1/4.$$

We found the analytical solution of this equation by rescaling the variable ρ and introducing a new function that allows to reduce it to the known Weber's equation [Weber, Math. Ann., 1, 1 \(1869\)](#).

We introduce new variable z as

$$\rho = e^{z-\alpha/\beta}, \quad (-\infty < z < \infty) \quad \Rightarrow \quad u_{K\lambda} = e^{z-\alpha/\beta} \Phi(z) \quad \Rightarrow \quad \frac{d^2 \Phi(z)}{dz^2} + [-\Delta^2 + V(z)] \Phi(z) = 0$$

$$\text{where } \Delta^2 = (K+1)^2 \text{ and } V(z) = -z\beta e^{2\alpha/\beta+2z}$$

Binding Energies of 2D Trions

In calculation of binding energies of X^- and X^+ trions we use electron and hole effective masses and for the screening length obtained by different ab initio methods: many-body G_0W_0 and GW density functional theory either in the local density approximation (LDA) or using the Perdew–Burke–Ernzerhof (PBE) functional

For molybdenum-based TMDCs

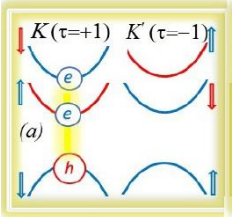
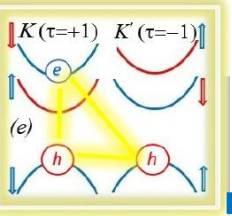
	Method	m_e/m_0	m_h/m_0	$r_0(A^0)$	X^- (mev)	X^+ (mev)
<p>MoS₂</p>	GW[10]	0.350	0.428	38.62[10]	32.80	33.2
	G_0W_0 [11]	0.6	0.54	38.62[10]	33.6	33.3
	LDA[12,13,14]	0.495	0.576	36.28[15]	34.2	34.4
	PBA[16,17,18,19]	0.47	0.575	44.69[17]	30.3	30.5
	HSE06[20]	0.37	0.44	38.62[10]	32.7	32.9
<p>MoSe₂</p>	GW[21]	0.38	0.44	51.71[22]	27.6	28.8
	G_0W_0 [11]	0.70	0.55	51.71[22]	31.7	31.3
	LDA[12,23,24]	0.59	0.686	39.79[15]	33.1	33.4
	PBE[12,17,18,25]	0.546	0.643	53.16[17]	28.4	28.5
	<p>MoTe₂</p>	G_0W_0 [11]	0.69	0.66	73.61[17]	21.3
LDA[24]		0.64	0.78	73.61[17]	21.9	22.4
PBE[25]		0.575	0.702	73.61[17]	20.4	20.7

Kezerashvili & Tsiklauri, *Few-Body Syst.* 58, 18 (2017).

Filikhin, Kezerashvili, Tsiklauri, & Vlahovic, *Nanotechnology* 29, 124002 (2018).

Binding Energies of 2D Trions

For tungsten-based TMDCs

	Method	m_e/m_0	m_h/m_0	$r_0(\text{Å}^0)$	X^- (mev)	X^+ (mev)
 WS ₂	GW[21]	0.27	0.32	37.89[22]	33.1	33.2
	G ₀ W ₀ [11]	0.44	0.45	37.89[22]	33.9	33.9
	LDA[12,23,24]	0.312	0.422	32.46[15]	37.4	32.6
	PBE[12,17,18,25]	0.328	0.402	40.17[17]	32.7	32.9
 WSe ₂	GW[21]	0.29	0.34	45.11[22]	28.3	28.4
	G ₀ W ₀ [11]	0.53	0.52	45.11[22]	30.2	30.2
	LDA[12,23,24]	0.36	0.476	34.72[15]	33.9	34.1
	PBE[12,17,18]	0.342	0.428	47.57[17]	27.1	27.2
WTe ₂	LDA[12]	0.325	0.46	49.56[15,26]	28.3	28.4
	PBE[27]	0.307	0.51	49.56[15,26]	27.6	28.2

The difference of the electron and hole masses gives appreciable uncertainty in the binding energies for X^- X^+

In monolayer TMDC material negatively and positively charged trions are bound

Kezerashvili & Tsiklauri, Few-Body Syst. 58, 18 (2017).

Filikhin, Kezerashvili, Tsiklauri, & Vlahovic, Nanotechnology 29, 124002 (2018).

Binding energy of bright trions

Binding energy of X^- and X^+ trions in WSe_2 , meV

Intravalley, singlet state, $L = 0, S = 1/2$

Freestanding Supported Encapsulated

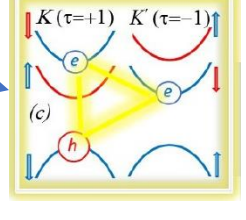
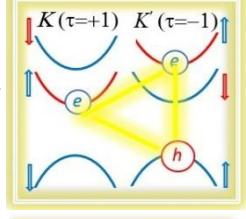
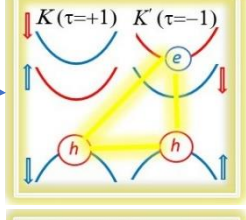
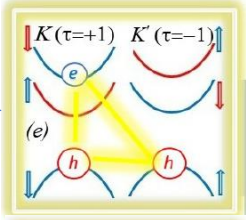
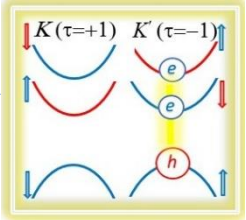
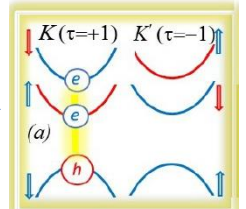
X^- , K valley electrons	38.7	34.6	29.4
X^- , K' valley electrons	28.6	21.4	18.2

Intervalley, singlet state, $L = 0, S = 1/2$

X^+ , K valley electron	29.4	24.5	21.6
X^+ , K' valley electron	28.0	22.9	19.8

Intervalley, triplet state, $L = 1, S = 3/2$

X^- , K valley electrons	26.3	20.1	18.7
X^- , K' valley electrons	-	-	-



WSe_2	m_{eK}/m_0	$m_{eK'}/m_0$	$\rho_0(\text{\AA}^0)$
	0.4[1]	0.36[1]	45.11[25]

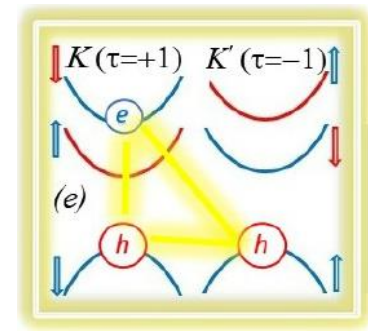
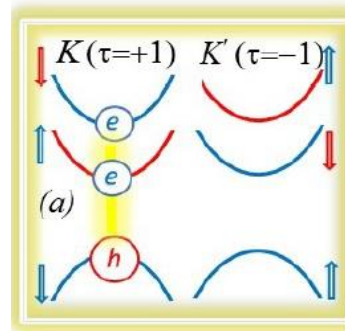
Electrons effective masses in WSe_2 are different in K and K' valleys, while effective masses of hole are the same

The singlet state intravalley X^- and intervalley X^+ trion binding energies

	Experiment	Theory	Freestanding		Supported		Encapsulated	
			X^-	X^+	X^-	X^+	X^-	X^+
MoS ₂	18±1[5],30[6],30,32[1]	29-31[33]	32.80	33.2	25.1	24.2	23.3	21.4
MoSe ₂	30[6,9]	29-31[33]	27.6	28.8	20.2	21.9	18.4	17.0
WS ₂	30[14],45[11]	28-30[33]	33.1	33.2	25.6	26.6	22.4	23.1
WSe ₂	30[7,8],29,35[20],	28-30[33],26±1[20]	28.6	28.9	21.4	22.9	18.2	19.8

Experiment

- [1] Kormanyos, et al. 2D Mater. 2, 022001 (2015).
- [5] K. F. Mak, Nat. Mater. 12, 207 (2013).
- [6] J. S. Ross, et al. Nat. Comm. 4, 1474 (2013).
- [7] Jones, et al., Nat. Nanotechnol. 8, 634 (2013).
- [8] Wang, et al., Phys. Rev. B 90, 075413 (2014).
- [9] Singh, et al.. Phys. Rev. Lett. 112, 21680 (2014).
- [11] Zhang, et al., Phys Rev. B 89, 205436 (2014).
- [14] Shang, et al., ACS Nano 9, 647 (2015).
- [20] Courtadeet al., Phys. Rev. B 96, 085302 (2017).



2D Biexciton

$$\Psi(\rho, \Omega_\rho) = \rho^{-\frac{2N-3}{2}} \sum_{\mu\lambda} u_\mu^\lambda(\rho) \Phi_\mu^\lambda(\Omega_\rho, \sigma),$$

hyperradius $\rho^2 = \sum_{l=1}^N x_l^2$, where x_l are Jacobi coordinates, and a set of angles Ω_ρ

where $\Phi_\mu^\lambda(\Omega_\rho, \sigma)$ are fully antisymmetrized functions with respect to two electrons and two holes in the case of the biexciton. These functions are constructed from spin function and the hyperspherical harmonics. The HH are the eigenfunctions of the angular part of the $2(N-1)$ -dimensional Laplace operator in configuration space with eigenvalue $L_N(L_N+1)$, where $L_N = \mu + (2N-5)/2$. f spherical harmonics and Jacobi polynomials.

$$\frac{d^2 u_\mu^\lambda(\rho)}{d\rho^2} + \left[\kappa^2 - \frac{L_N(L_N+1)}{\rho^2} \right] u_\mu^\lambda(\rho) = \sum_{\mu'\lambda'} V_{\mu\mu'\lambda\lambda'}(\rho) u_{\mu'}^{\lambda'}(\rho),$$

where

$$V_{\mu\mu'\lambda\lambda'}(\rho) = \frac{2M}{\hbar^2} \int [\Phi_\mu^\lambda(\Omega_\rho, \sigma)]^* \left(\sum_{i<j} V_{ij} \right) \Phi_{\mu'}^{\lambda'}(\Omega_\rho, \sigma) d\Omega_\rho$$

is the N -particle effective potential energy defined by the Keldysh potential V , $\kappa^2 = 2M B/\hbar^2$, where B is the binding energy, and M is a reduced mass for biexciton.

Table 2 Experimental and theoretical results for biexciton binding energies in meV for TMDCs materials

TMDC	Present work	Experiment	SVM [18,19]	PIMC [21]	DFT and PIMC [20]	DMC [22]
MoS ₂	22.1	40, 60 [14], 70 [11]	22.5		22.7	22.7
MoSe ₂	17.9	~20 [12]	18.4		19.3	17.7
WS ₂	23.1	45 [4], 65 [5]	23.6	21	23.9	23.3
WSe ₂	19.8	52 [13]	20.2		20.7	20.0

SVM stochastic variational method, *PIMC* path integral Monte Carlo method, *DFT and PIMC* density functional theory and path integral Monte Carlo method, *DMC* diffusion Monte Carlo method

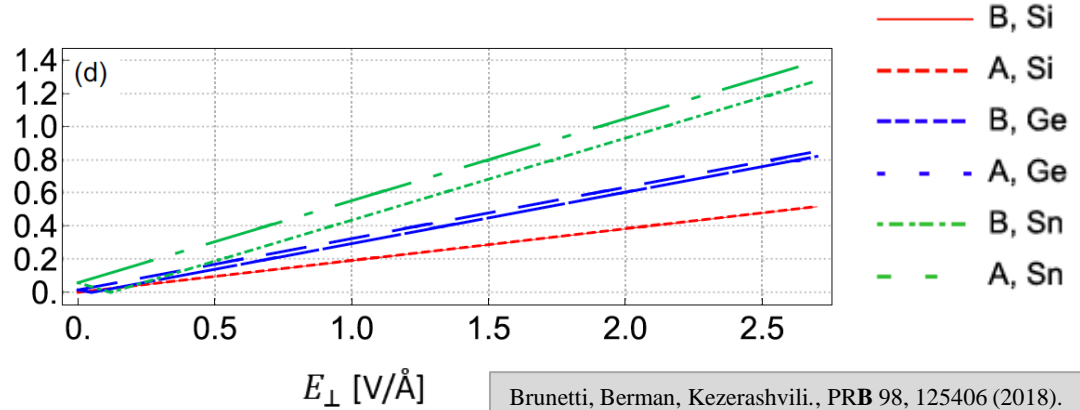
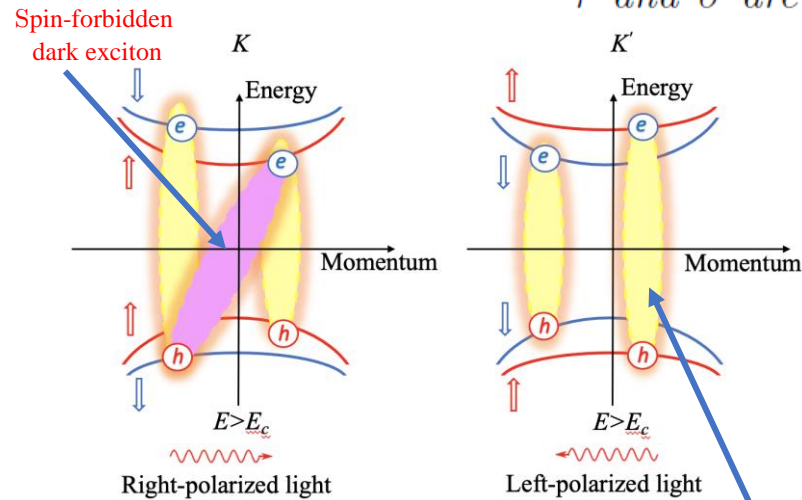
Kezerashvili & Tsiklauri, Few-Body Syst. 58, 18 (2017).

Electron and hole masses in Xenes

$$\hat{H} = v_F (\xi p_x \hat{\tau}_x + p_y \hat{\tau}_y) - \xi \Delta_{gap} \hat{\sigma}_z \hat{\tau}_z + \Delta_z \hat{\tau}_z$$

$\xi, \sigma = \pm 1$ are the valley and spin indices, $\Delta_z = ed_0 E_{\perp}$

$\hat{\tau}$ and $\hat{\sigma}$ are the pseudospin and real spin Pauli matrices



Brunetti, Berman, Kezerashvili., PRB 98, 125406 (2018).

Bright excitons correspond to the lowest optically induced transition between the bands of the same spin at the K and K' point

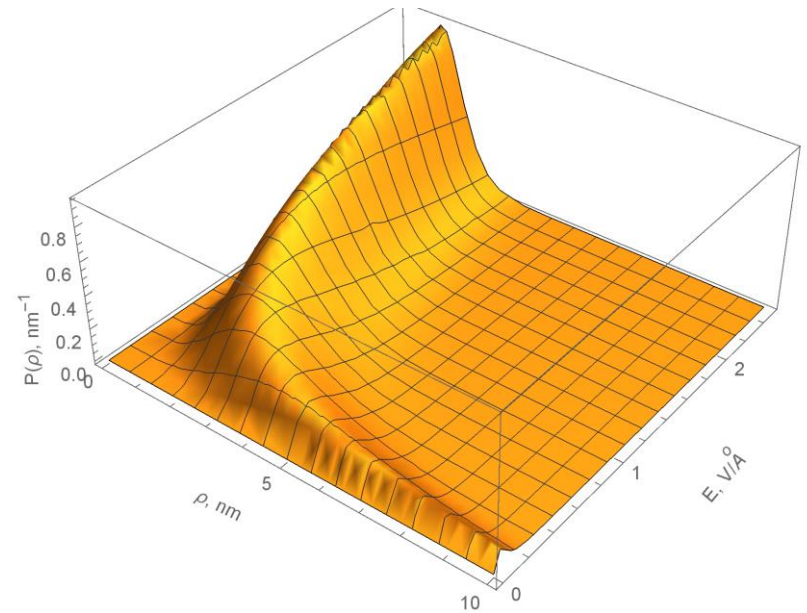
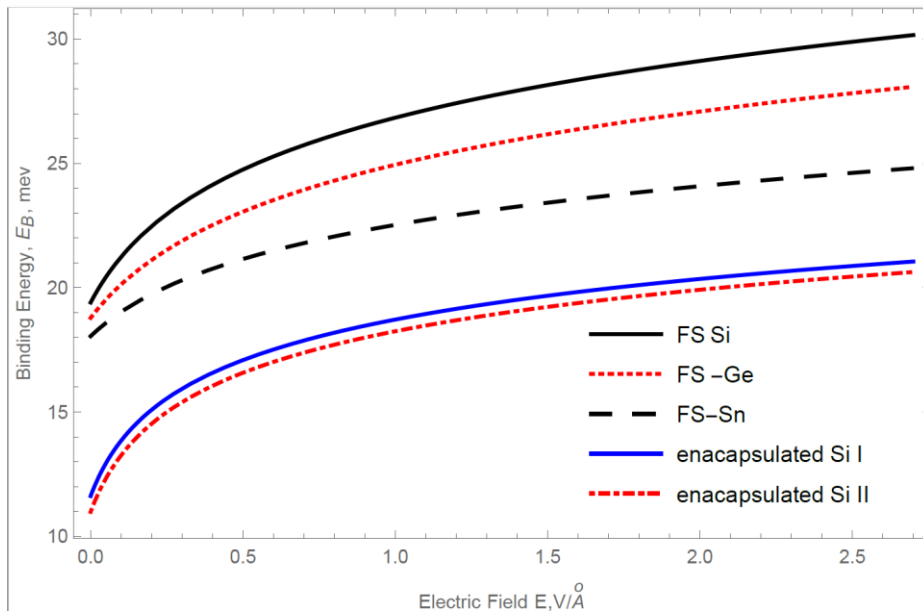
$$m = \frac{|\xi \sigma \Delta_{so} - ed_0 E_{\perp}|}{v_F^2}$$

- $E_{\perp c} = \frac{\Delta_{so}}{ed_0}$
- d_0 is the buckling parameter
- $\xi, \sigma = \pm 1$ – the valley and spin indices
- $\xi = -\sigma$ – large gap – A exciton
- $\xi = \sigma$ – small gap – B exciton

- Values of μ of A and B excitons in Ge and Si do not differ much.
- Difference between of A and B excitons in Sn does not produce significant difference in the binding energies.

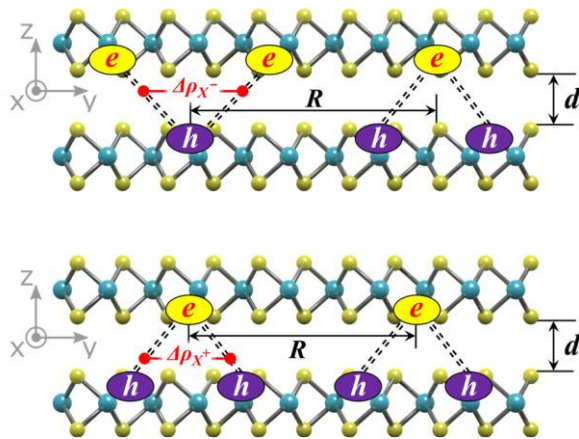
In Xenes, calculations are done for A excitons.

Trions in Xenon

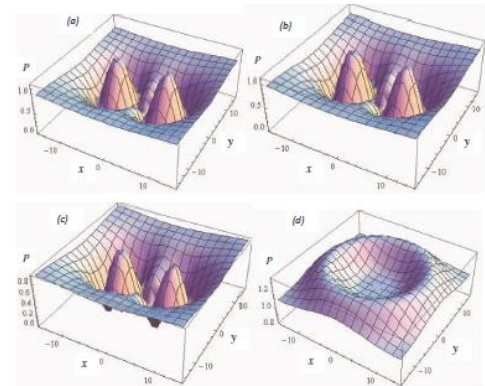
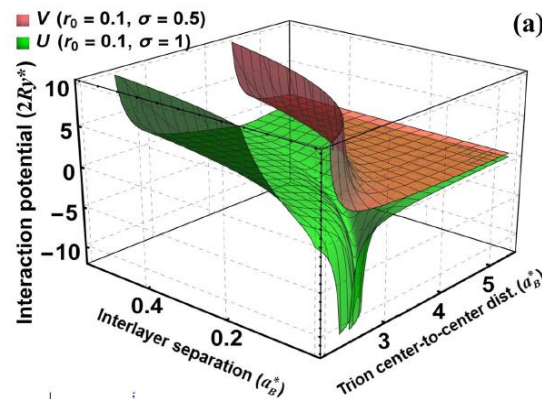


Strongly correlated coherent states of excitons have been the subject of intense theoretical and experimental studies. This topic has recently boomed due to new emerging quantum materials such as van der Waals heterostructure, with bound atomically thin layers of transition metal dichalcogenides.

We analyze the collective properties of interlayer trions in TMDC heterostructures and predict strongly correlated phases—crystal and Wigner crystal—that can be selectively realized with TMDC heterostructure of properly chosen electron-hole effective masses and by varying their interlayer separation distance.



Charged interlayer exciton structure



Conditional probability distribution

- *Berman & Kezerashvili, Few-Body Syst (2011) 50, 407*
- *Berman, Kezerashvili, & Tsiklauri, J. Mod. Phys. B 28, 1450064 (2014).*
- *Bondarev, Berman, Kezerashvili & Lozovik, Comm. Phys, (2021) 4:134*

Let's set of new variable

$$w = S(z - z_0), \quad \text{where } S = \sqrt[4]{4\beta e^{(2\alpha - \beta)/\beta}}$$

$$\frac{d^2\Phi(z)}{dZ^2} + [-\Delta^2 + V(z)]\Phi(z) = 0 \quad \longrightarrow \quad \left[\frac{d^2\Phi(z)}{dw^2} + \frac{-\Delta^2 + 1/8S^4}{S^2} - \frac{1}{4}w^2 \right] \Phi(w) = 0$$

This equation is square-integrable only if

$$\frac{-\Delta^2 + 1/8S^4}{S^2} = \frac{(2n + 1)}{2}, \quad n = 0, 1, 2, \dots$$

This equation will be reduced to the following biquadratic equation

$$S^4 - 4(2n + 1)S^2 - 8\Delta^2 = 0, \quad n = 0, 1, 2, \dots \quad \xrightarrow{\text{solution}} \quad S^2 = 2(2n + 1) + 2 \left[(2n + 1)^2 + 2\Delta^2 \right]^{1/2}$$

$$2\beta e^{(2\alpha - \beta)/2\beta} = 4 \left((2n + 1) + \left[(2n + 1)^2 + 2\Delta^2 \right]^{1/2} \right)^2$$

$$E = -\frac{ke^2}{\epsilon\rho_0} \ln \rho_0 + B_{123} + \mathcal{J}_{K\lambda K\lambda} + \frac{ke^2}{\epsilon\rho_0} \left\{ 1 + \ln \left[\frac{[n + 1/2 + \sqrt{(n + 1/2)^2 + \Delta^2/16}]^2}{\frac{2\mu}{\hbar^2} \frac{ke^2}{\epsilon\rho_0}} \right] \right\}, \quad n = 0, 1, 2, \dots$$

$$\Phi = D_n(w) = 2^{(n-1)/2} e^{-w^2/4} F\left(\frac{1-n}{2}, \frac{3}{2}, \frac{w^2}{2}\right), \quad F\left(\frac{1-n}{2}, \frac{3}{2}, \frac{w^2}{2}\right) \text{ is a confluent hypergeometrical function.}$$

Summary

The binding energies of the trions are calculated for different bulk materials based on the Faddeev equation for AAB system in configuration space. It was found that the binding energy of *negative trion* is relatively small, while the *positive trion* is unbound.

Calculations within the method of hyperspherical harmonics show that in 2D monolayer TMDC semiconductors due to the reduced dimensionality *negatively and positively charged trions* are bound and the binding energy of positive trion is always greater than for the negative trion

Our studies raise the possibility of controlling the binding energies of trions in Xenon monolayers using the external electric field and open the additional degree of freedom to tailor the binding energies of trions

I wish to thank my co-authors

Dr. Igor Filikhin

Anastasia Spiridonova

Dr. Shalva Tsiklauri

Prof. Branislav Vlahovic

Thank you!